

**Rainfall-Runoff Modelling for Flash Floods in
Cuong Thinh Catchment; Yen Bai Province:
Vietnam**

Ezra Pedzisai
March, 2010

Rainfall Runoff Modelling for Flash Floods in Cuong Thinh Catchment; Yen Bai Province: Vietnam

by

Ezra Pedzisai

Thesis submitted to the International Institute for Geo-information Science and Earth Observation in partial fulfilment of the requirements for the degree of Master of Science in Geo-information Science and Earth Observation, Specialisation: Geo-Hazards

Thesis Assessment Board

Dr. D.G. Rossiter (Chair)

Dr. R. van Beek (External Examiner)

Dr. D. Alkema (First Supervisor)

Prof. Dr. V. G. Jetten (Second Supervisor)

Ms Nguyen, T. H. V. (Thesis Advisor)

Observer :

Drs. T. M. Loran (Programme Director)



**INTERNATIONAL INSTITUTE FOR GEO-INFORMATION SCIENCE AND EARTH OBSERVATION
ENSCHEDA, THE NETHERLANDS**

Disclaimer

This document describes work undertaken as part of a programme of study at the International Institute for Geo-information Science and Earth Observation. All views and opinions expressed therein remain the sole responsibility of the author, and do not necessarily represent those of the institute.

Abstract

An assessment of the generation of runoff from severe rain events and flood propagation was carried out on a 15km² *Cuong Thinh* catchment in Yen Bai province, north-western Vietnam. *Cuong No* stream passes through the flash flood prone Yen Bai town towards the Red River confluence. Two distributed catchment models were coupled; LISEM, event-based 1D hydro-dynamic rainfall-runoff model with SOBEK, a 2D hydraulic flood propagation model using a characteristic high intensity short duration storm. LISEM simulated two runoff scenarios, one on a whole catchment hydrograph which was compared with SOBEK normal slope scenario. Secondly, 34 sub-catchments hydrographs were simulated and incorporated into the three SOBEK complex terrain scenarios namely; dike-break on terraced slopes, terraced slopes only and normal slope in the rice fields. On the one hand, using LISEM model, it was observed that the main stream sub-catchment upslope of the rice fields contributes immensely to the catchment runoff. On the other hand, results simulated on The whole catchment scenario revealed a short lag as a fast catchment response to severe rainfall despite high interception due to dense forest and plantation cover and important surface storage by numerous ponds in the catchment. Severe tropical monsoon storms initiate a kinematic wave on the upslope which is propagated as a flood wave upon entering the rice fields as the SOBEK scenarios confirmed. A runoff coefficient of 0.44, three hour duration and peak discharge of up to 140m³/s was the main result of the LISEM whole catchment scenario. However, the SOBEK scenario predicted 20m³/s peak discharge. The SOBEK scenarios indicated that on one hand dikes play an important role in storing the runoff during the initial stages. On the other hand, they overtop and break thereby initiating a flood wave that propagates down-slope in the terraced rice fields. Breaking dikes led to doubling the flood peak which prois propagated as one wave unlike in the other two scenarios showed two subdued flood peaks separated by a few hours. During a dike-break situation the flood extent highest while the flood depth was consistent in all three scenarios. In these flood scenarios complex topography in the rice fields has an important buffering and storage function by the dikes, inter-field ridges and natural 'bottlenecks'. Natural 'loops' in the rice field edges help to break the flow velocity while the bottlenecks act as the 'hydrological valves' regulating flow from the rice fields. While the two models predict a similar volume of flow generated in the catchment, LISEM predicted an earlier flood peak and shorter high flow duration while SOBEK predicted a longer duration of the event. The results imply a shorter warning time in both models although LISEM predicted an earlier and higher peak flow than the SOBEK scenarios. The coupling of LISEM and SOBEK was crucial to understand catchment behaviour on a complex terrain.

Acknowledgements

I am greatly indebted to the following for the progress of this study. The Dutch government for the fellowship according me this opportunity to learn in such a prestigious institution of international repute. ITC for the professional and academic development, nurturing and developing a passion for the best and hard work.

I was greatly privileged to work under the supervision of Dr D. Alkema and Professor V. G. Jetten. The ideas were critical and crucial to the developments that took place through the research phase. My first supervisor Dr D Alkema for the unwavering support and informed guidance who helped me shape and develop ideas supervisors with a very thorough review and ensuring the progress was on track. Professor Jetten, for the consistent reviewing and updating of the model versions to give the best I could get in the shortest of time in addition to his consistent supervision. The thesis advisor, Nguyen Hai Van has been the critical reference point, shaping my ideas and conception of the problem, the consistent updating and also supplying some of the data needs. The field guidance and logistics as well as continued support in this work is acknowledged. Dr Smeth for the support and guidance during the laboratory experiments. The staff in the AES who worked with me in all times, the course director, Drs Tom Loran and the course secretary Anneke. Mr G. Parodi for helping identify suitable event storm candidate.

To my colleagues in the AES department, geo-hazards programme and in modelling. The team work was great Tarik, Niranga, Namratha, Sheika, and Trang. Your support was huge and I express my gratitude to the support rendered, Janack my friend thank you for the effort on your support of my field work. Colleagues, Dita, Gopi, Lekoko, Ashebir, Leta, Andre, Paula, Melanie, Nadira. For guidance from Mhosisi Masocha Alain Pascal Francis, Abel Ramoelo, is greatly appreciated.

To the Zimbabwean community; Pedzisai Kowe, Webster, Donald, Upenyu, Juliet, Shelton, Patience, Chenai, Florence and Sydney and the rest not mentioned here for support and prayers everyday for me. Everyone else who has not been mentioned in this text, I appreciate your support, the space is too small.

Last but the greatest I am grateful to my wife, Sunungurayi and my children; Tawananyasha, Rutendo and Rejoice, who soldiered on and endured a home without a father. Thank you. To my parents Mr and Mrs Pedzisai, my brothers and sisters, your support is greatly appreciated.

Dedication

This thesis is dedicated to my dear wife; Sunungurayi, my son; Tawananyasha and daughters; Rutendo and Rejoice.

Table of contents

1. Introduction	13
1.1. Background	13
1.2. Statement of the problem.....	13
1.3. Main objective	14
1.3.1. Specific objectives.....	14
1.4. Main reseach question	14
1.4.1. Specific questions.....	14
1.5. Hypothesis	14
1.6. Justification.....	14
1.7. Study area	15
1.7.1. Background of the study area	15
1.7.2. Drainage	16
1.7.3. Rainfall	16
1.7.4. Geomorphology and soils.....	17
1.7.5. Land uses	18
1.8. Structure of the thesis	18
2. Literature review	19
2.1. Introduction.....	19
2.2. Runoff generation processes.....	21
2.3. Factors controlling runoff	21
2.4. Hydrographs.....	23
2.5. Classification of floods	23
2.6. Factors influencing flash floods	23
2.7. Characteristics of flash floods	24
2.8. Flash flood prediction and forecasting	25
2.9. Modelling.....	25
2.9.1. Modelling approaches	26
2.10. Conclusion	28
3. Methodology and data.....	29
3.1. Introduction.....	29
3.2. Data requirements of LISEM and SOBEK.....	29
3.2.1. LISEM data requirements.....	29
3.2.2. SOBEK data requirements	31
3.3. Pre-field work Inventory	32
3.4. Field work data collection	32
3.4.1. Mapping land use	32
3.4.2. Sampling strategy	32
3.4.3. Cross sections	34
3.4.4. Water bodies.....	34
3.4.5. Rice paddy elements: Dikes, terraces and ‘ridges’	34
3.4.6. Discharge.....	36

3.4.7.	Interviews	37
3.4.8.	Secondary data.....	37
3.5.	Post field work data processing	37
3.5.1.	Soil physical properties	37
3.5.2.	DEM for LISEM and SOBEK.....	42
3.5.3.	Land use.....	42
3.5.4.	Surface roughness.....	42
4.	Modelling and Results.....	44
4.1.	Introduction.....	44
4.2.	LISEM Modelling Scenarios	44
4.2.1.	Sub-catchments (34) scenario.....	45
4.2.2.	Whole catchment scenario.....	45
4.3.	Sensitivity analysis.....	46
4.4.	Calibration	46
4.5.	Simulation	46
4.6.	LISEM results	47
4.6.1.	Runoff coefficient.....	47
4.6.2.	Sub-catchment hydrographs	47
4.6.3.	Sub-catchment C01 scenario	49
4.7.	SOBEK model.....	49
4.7.1.	Sobek scenarios	49
•	Dike-break scenario	49
•	Terraced slope scenario	50
•	Normal slope scenario.....	50
•	C01 scenarios	50
4.8.	Schematisation	50
4.8.1.	Cross sections	51
4.8.2.	Boundaries.....	52
4.8.3.	Initial water level.....	52
4.8.4.	Dike breaks	52
4.9.	Sobek model results	54
4.10.	Topographic scenarios	54
4.10.1.	Flood Depth and Extent	54
4.10.2.	Maximum Flow Velocity	55
4.10.3.	Maximum Impulse.....	56
4.11.	SOBEK flash flood scenario hydrographs.....	58
4.12.	Catchment Water Balance.....	58
4.13.	Applicability of LISEM as a Flash Flood Prediction Tool.....	60
4.14.	Influence of the C01.....	62
4.15.	Summary	63
5.	Discussion, conclusions and recommendations.....	64
5.1.	Discussion	64
5.2.	Conclusions.....	66
5.3.	Recommendations.....	67

5.4. Limitations of the study67

List of Figures

Figure 1.1: Map of the study area	15
Figure 1.2: Mean monthly rainfall for Yen Bai for (1960 – 2008).	16
Figure 1.3: Gumbel plot of the maximum daily rainfall for Cuong Thinh area.	17
Figure 1.4: Geomorphology (a) and the lithology (b) of the area	17
Figure 2.1: Rainfall-runoff processes.....	20
Figure 2.2: Runoff generation process.	21
Figure 3.1: Study methodology	29
Figure 3.2: LISEM rainfall-runoff module	30
Figure 3.3: SOBEK model; pre-simulation, simulation and results blocks.	31
Figure 3.4: Spatial distribution of soil samples by soil texture.....	33
Figure 3.5: Spatial distribution of soil samples by land use	33
Figure 3.6: Points of cross section and discharge measurement.	33
Figure 3.7: Cracks on dikes and ponds	35
Figure 3.8: View of terraces (a) and the measurement of height (b) and width (c).....	35
Figure 3.9: Factors in the calculating the water level using equation (3.1).	36
Figure 3.10: Ksat field experiment.....	38
Figure 3.11: Histogram (a), boxplot (b) and quantile-quantile plot (c) for Ksat.....	40
Figure 3.12: Box plots for Ksat by texture class (a) and land use class (b).....	40
Figure 3.13: Pairwise scatterplot of soil parameters	41
Figure 3.14: Soil physical properties.....	41
Figure 3.15: DEMs; upslope (a) and whole area (b) for LISEM and the dike-break DEM for SOBEK (c).	43
Figure 3.16: Water bodies (a) and the respective land uses (b) in the study area.....	43
Figure 4.1: Model interface Figure 4.2: Rainfall event	45
Figure 4.3: Simulation results as a screen shot.	47
Figure 4.4: Contribution of sub-catchments to the discharge into the rice fields.	48
Figure 4.5: SOBEK scenario profiles.....	50
Figure 4.6: Cross section node (a), shape and geometry (b) and the location details (c)	51
Figure 4.7: 1D boundary node (a), boundary condition definition (b) and discharge table (c).....	52
Figure 4.8: Dike-break node (a), node definition (b) and dike-break timetable (c).....	52
Figure 4.9: Initial water level input tab (a) and its node (b) for each simulation.....	52
Figure 4.10: Three dikes with dike-break nodes (red stars) before (a) and after (b) the dike-break (b).	53
Figure 4.11: Schematisation of the model (a) and enlarged view of the middle rice field (b).	53
Figure 4.12: Maximum depths (m) simulated with three SOBEK surface terrains.....	55
Figure 4.13: Flood extent (a) and flood depth.....	55
Figure 4.14: shows the distribution of the maximum velocity by flood scenarios.....	57
Figure 4.15: Impulse with respect to the three scenarios.	57
Figure 4.16: Hydrographs for the three SOBEK flood scenarios.....	58
Figure 4.17: showing the water balance in the catchment with respect to the three scenarios.	59

Figure 4.18: Cumulative volume at the downstream boundary for the three SOBEM scenarios.59
Figure 4.19: Hydrographs for SOBEM, LISEM whole catchment and C01 scenarios.....60
Figure 4.20: Comparison of the predicted cumulative volume for the two models.....61
Figure 4.21: Infiltration influence on predicted volume61
Figure 4.22: C01 effect on the volume outflow for the three scenarios.....62

List of tables

Table 3.1: Input parameters for LISEM rainfall-runoff modelling.	30
Table 3.2: Input parameters for SOBEK flood propagation modelling	31
Table 3.3: Inventory of data.....	32
Table 3.4: Sampling strategy for soil samples.....	32
Table 3.5: Rainfall data for study area	37
Table 3.6: Ksat (mm/h) by land use class.....	39
Table 3.7: The land use based manning's n values used in the flood modelling	42
Table 4.1: Results of Ksat Sensitivity to the rainfall-runoff model.	46
Table 4.2: Summary of the total nodes used to schematise the model.....	51
Table 4.3: Summary of flash flood simulation results	54

1. Introduction

1.1. Background

Vietnam has a tropical monsoon climate that is associated with severe storms triggering floods. Flooding due to storms is regular problem in the Indo-Chinese region including Thailand, China and Vietnam. An annual average of at least five typhoons and tropical low-pressure events are recorded in Vietnam occurring between July and October (Imamura and To, 1997). This implies that the life, well-being and livelihood of the community is affected occasionally due to the floods including the north western mountainous area of Yen Bai. Upon this recognition, the Government of Vietnam has made institutional arrangements entrusting the Deputy Prime Minister for Flood and Storm Control to handle floods disaster management with the help of a Central Steering Committee that works with representatives of relevant ministries and agencies. A Disaster Management Working Group also worked in the province due to the flooding problems.

A recent tropical storm (Kammuri) that hit mainland Vietnam on the 8th through the 13th of August 2008 affecting seven provinces including Yen Bai (Duong and Nguyen, 2008) reinforced the need for action on the areas affected. This storm resulted in many deaths, evacuations resulting from loss of basic necessities. Yen Bai province was one of the most hard-hit with many deaths and reported injuries caused by flooding and became inaccessible due to storm triggered floods (Duong and Nguyen, 2008). The area became inaccessible due to infrastructural damage, making food aid and other emergency relief items difficult to obtain. Over a thousand travellers the majority being tourists en route to Sapa, got stranded in Yen Bai as a result of flood related transport problems (Duong and Nguyen, 2008). A joint rapid assessment after the flood disaster also reported huge losses in Yen Bai Province. The resultant losses due to the occurrence of this flood hazard included deaths and injuries of people and animals, destruction of physical infrastructure and critical facilities, loss of basic necessities and cropland valued at over 400 billion local currency (Vietnamese dong) which amounts to about 21 million USD.

In Vietnam, models (rainfall–runoff and conceptual) and methods (correlative and regression) have been used largely in short-range hydrological forecast (Duong and Nguyen, 2008). Hydrological and hydraulic models have also been used for forecasting flood downstream areas for bigger rivers with 70 to 80 percent of the amount of rainfall and runoff occurring 3 - 6 months in the rain season (Imamura and To, 1997).

1.2. Statement of the problem

Extreme monsoon storms trigger flash floods in NW Vietnam. Yen Bai City, on the downstream side of a small size catchment tributary to the Red River, is especially susceptible to floods. The town has a big concentration of people, physical infrastructure and socio-economic activities. The rainfall-runoff relationship in this catchment is not well understood yet it is important to plan for mitigation of

subsequent flood damages. A good understanding of the rainfall-runoff relationship is also important for predicting the prominent flash floods in the catchment.

Major land uses in the catchment include tea growing and tree plantations on hill-slopes. Rice cultivation on paddies on gentler terrain and valleys. Hill slopes with weathered clays tend to have more clay texture than the regularly tilled valley soils and the respective infiltration characteristics have to be understood. On the other hand, rice cultivation has complex man-made terrain features including small dike structures that storage water but may break during large storms to exacerbate flooding. Moreover, the hydrological influence of these land uses in contribution to the generation and propagation of huge runoff amount to result in flash floods on the catchment had to be understood since flash floods are a persistent problem in the area.

1.3. Main objective

To gain better understanding of flash flood propagation in the Cuong Thinh catchment

1.3.1. Specific objectives

- 1 to assess the land use and soil physical properties in the catchment
- 2 to identify the specific role of the rice paddies and upslope land uses in the catchment hydrological system
- 3 to test the applicability of LISEM rainfall-runoff in combination with Sobek flood propagation model to explain flash floods in this area

1.4. Main reseach question

What are the trigger mechanisms of flash flood propagation in the Cuong Thinh Catchment?

1.4.1. Specific questions

- 1 What are the land use and soil physical properties in the catchment?
- 2 What is the contribution of the up slope and the rice paddies land uses in the runoff generation and propagation of the flash floods?
- 3 How applicable is the LISEM in combination with Sobek to model flash floods in this catchment?

1.5. Hypothesis

Rice fields play a key role in the propagation of flash flood in the catchment under storm events.

1.6. Justification

Flash floods lead to loss of human life, disrupt social and economic activities. Key to effective disaster management actions is the need to understand the mechanisms of high flow runoff generation that lead to flash floods. The land uses and soil physical properties influencing the catchment hydrology of the area

needed to be assessed. Therefore, modelling runoff generation and flood propagation requires tools capable of physically quantifying these events at the catchment scale. It is important first to understand the hydrological processes responsible for runoff generation through hydrologic modelling and then propagation of the flood using an appropriate flood model. Catchment physiographic, hydrological and space-time variation parameters are to be appraised as well as the underlying soil physical properties and land use characterised.

1.7. Study area

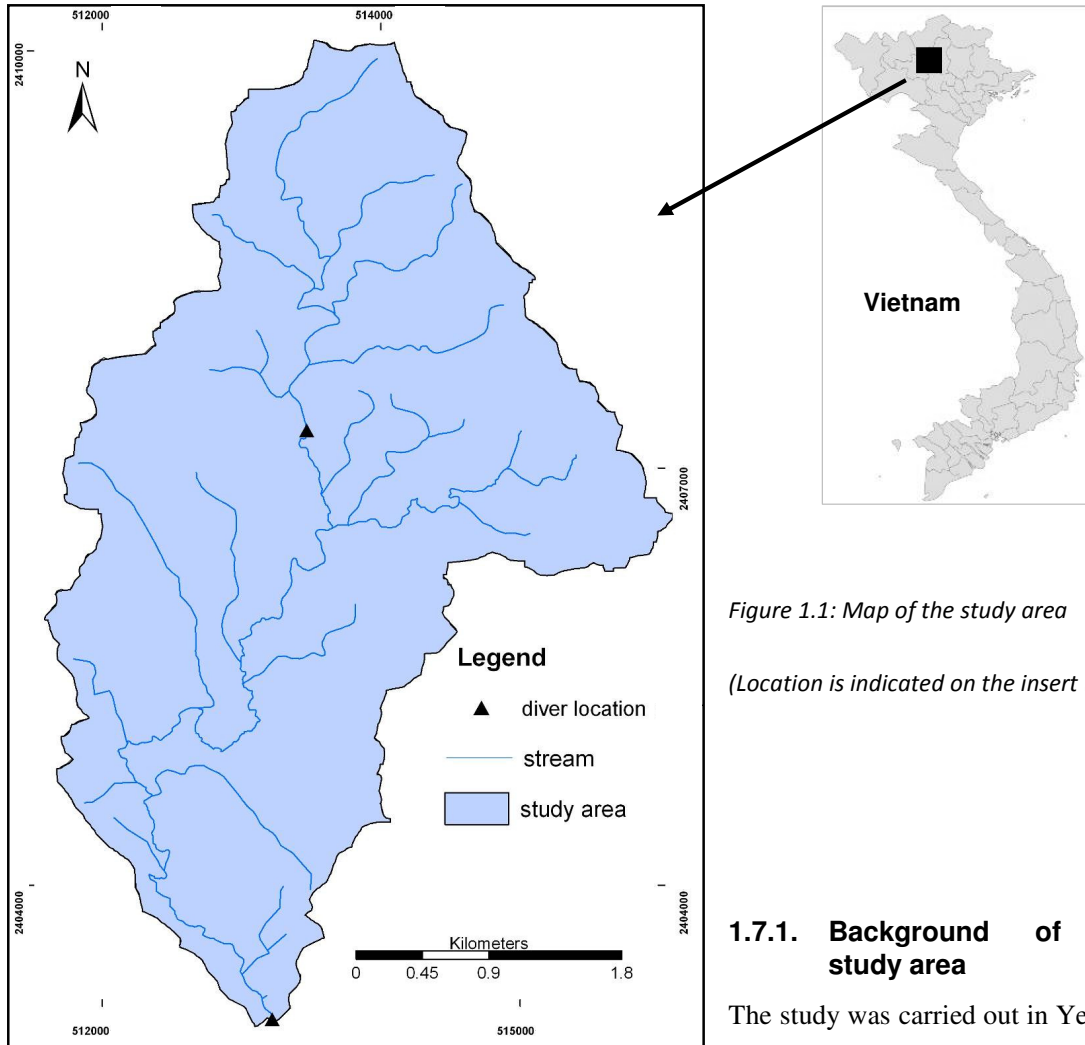


Figure 1.1: Map of the study area
(Location is indicated on the insert (top)).

1.7.1. Background of the study area

The study was carried out in Yen Bai Province, north western of Vietnam, a country in South East Asia, as shown on Figure 1.1. This longitudinal-shaped catchment covers the three ‘communes’ largely *Cuong Thinh*, *Nam Cuong* and partly *Minh Bao* on the north, south and north-eastern parts respectively. The catchment has a characteristic mountainous landscape with rolling terrain with predominantly rural land uses. The area lies between 30 and 330m elevation above the local datum. The catchment is covers 15.5km².

1.7.2. Drainage

The drainage comprises ‘*Cuong No*’ stream originating in the northern hilly areas on a southward direction. As shown on Figure 1.1, the main stream winds at the centre on its southward drainage. ‘*Cuong No*’ Stream, which is one of the five important tributaries of the Red River, inundates the town’s residential and industrial areas. The main tributaries of the *Cuong No* Stream join from the eastern and north western sides forming a dendritic drainage pattern with several bottlenecks where the river channel incised across higher elevation features. In the valley areas on the centre of the study area, small concrete and clay canals drain excess water from the rice fields.

1.7.3. Rainfall

The area has tropical semi-humid climate characteristics with rainfall monthly as shown on Figure 1.2. The area receives rainfall throughout the year as presented on Figure 1.2. However, a characteristic monsoon season showing high rainfall activity of over 150mm in one month begins in May through October. This period is also the active typhoon season characterised by moisture-laden monsoon winds from the Pacific Ocean occasionally causing severe storms leading to flash floods. The maximum rainfall amount is expected around August as shown on Figure 1.2.

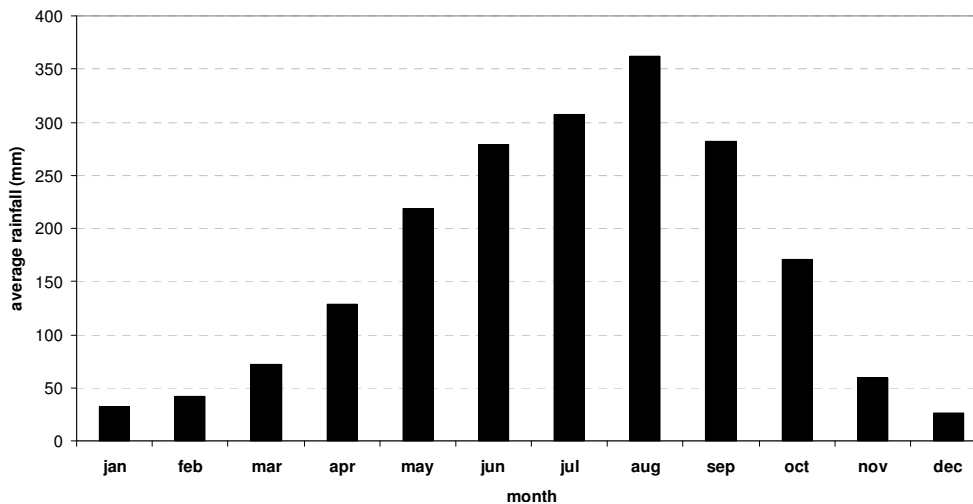


Figure 1.2: Mean monthly rainfall for Yen Bai for (1960 – 2008).

The respective Gumbel plot of the extreme events based on annual maximum daily data (1960 – 2008) is shown on Figure 1.3. A seven hour rainstorm of second September 2007 with 125.9mm of which 120mm depth occurred in only two hours is as estimated on the plot with thick arrows.

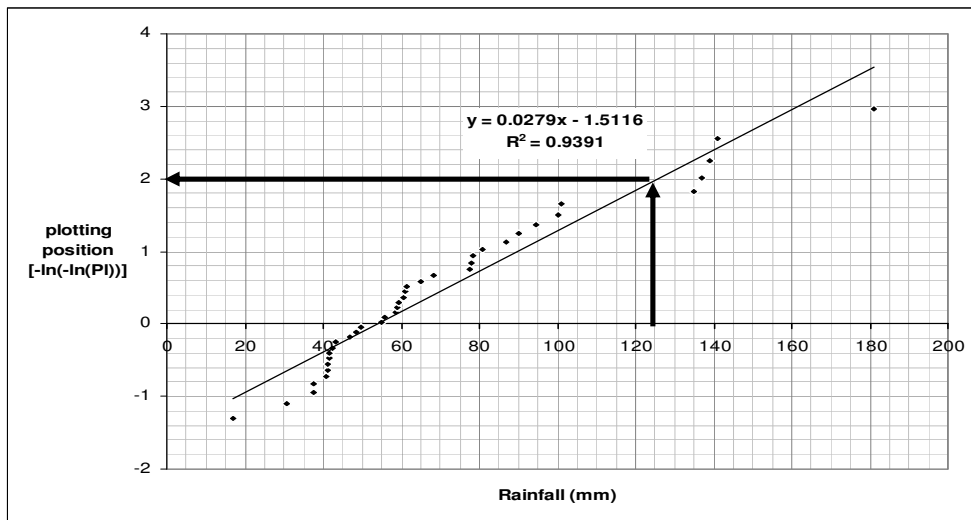


Figure 1.3: Gumbel plot of the maximum daily rainfall for Cuong Thinh area.

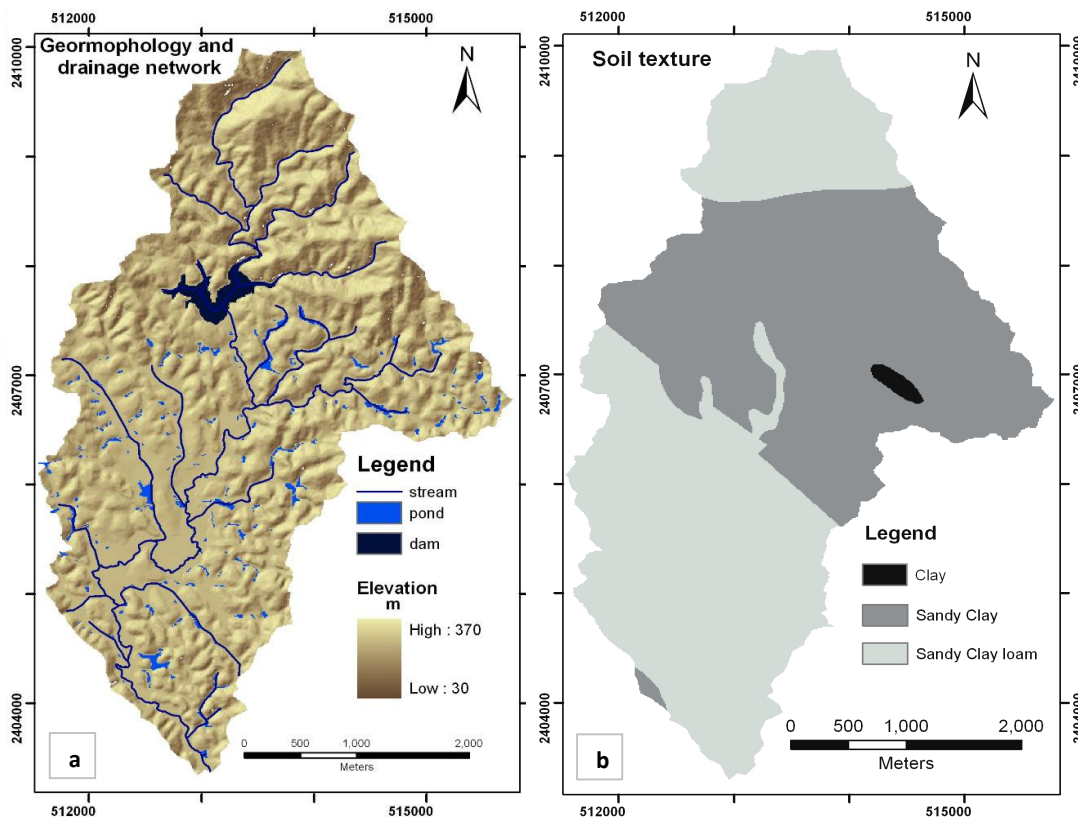


Figure 1.4: Geomorphology (a) and the lithology (b) of the area

1.7.4. Geomorphology and soils

The area is highly rugged with steeper mountainous northern area where the main river originates. The central part is low lying valley that winds through the rugged terrain area where the slope is nearly level and the land use predominantly rice and other valley crop farming. The geomorphology of the area is as shown on Figure 1.4a with rugged terrain on the fringes of the area and almost

levelling floors of the valleys. The area constitutes sandy clay and sandy clay loam soil textures. Hilly areas are more clayey while valleys are sandy to silt in texture. A map of the soils in the study area is shown on Figure 1.4b.

1.7.5. Land uses

The study area has agriculture and plantations as major land uses. Dense forests, mixed tree plantations and tea fields on slopes constitute a common higher slopes land use while the valley floors are primarily rice fields under terraced slopes with dikes, ponds and roads crossing the fields. The dikes and roads are made of clay characterised by dense trees. Map of land uses is presented on Figure 3.5.

1.8. Structure of the thesis

Chapter 1: introduced the study by defining the flash flood problem, specifying objectives and their related questions. The study area is also introduced in this chapter.

Chapter 2: outlines the literature reviewed in the thesis. It explores the processes and link between rainfall-runoff relationship and flash floods propagation in complex terrain.

Chapter 3: outlines the methodology employed in the study to answer the proposed research questions and the data collection. Soil data processing, analysis and results to create data base for LISEM rainfall-runoff model.

Chapter 4: presents the modelling of two scenarios in LISEM and three in SOBEK. The respective results from the two models are also presented in this chapter.

Chapter 5: presents the discussion, conclusions and recommendations from the study.

2. Literature review

2.1. Introduction

The prediction of flash floods is problematic for decades yet the floods are complex and sporadic. Understanding this problem in *Cuong Thinh* catchment is important especially in the view of the complex topography of the rice fields.

The relationship between rainfall and runoff has been subject of research over a long time. Sorooshian (1997) highlighted that rainfall-runoff modelling started as an engineering hydrology preoccupation, driven by societal needs for structural design purposes and more importantly, to address operational requirements including flood forecasting. However, each catchment has a unique runoff response to different rainfall events. Modelling is relevant to understand rainfall-runoff and flash flood behaviour especially in areas susceptible to flash floods. Floods have been defined as when a body of water has risen, overflowing the channel to adjacent areas which are normally not inundated (Ward, 1978 in Dhar and Nandargi (2003)). Therefore flash flood is a sudden rise of the flow to overflow the river banks within a short period of time since onset of the causing rain event. Norbiato et al (2008) noted the time to be within minutes to a few hours, with the maximum being 24 hours according to the Flash Flood Guidance. This has implications on warning time which becomes extremely very short if a catchment responds rapidly to rainfall. Flash floods are also recognized as local phenomena of less than a few hundred square kilometres, resulting from intense rainfall, on steep slopes, and impermeable surfaces, saturated soils, or anthropogenic forcing (Norbiato et al, 2008). Many models try to simulate runoff from rainfall. However, the general consensus is that when rainfall input exceeds losses such as interception, infiltration evaporation and surface storage, runoff is generated.

The crux in understanding flash floods is knowledge of how a catchment responds to severe rainfall events. Therefore, a channel flow hydrograph showing the hydrological response of a system to rainfall is simulated in rainfall-runoff modelling (Rientjes, 2004). Implicitly, a hydrograph is an indispensable tool for better understanding of flash floods in a catchment. The rainfall-runoff model discharge hydrograph is also important in flood modelling for flood propagation in an area. The relevant characteristics derived from a hydrograph that are useful as effecting damages include duration, lag time, time to peak discharge, peak discharge, rate of rising, flow velocity and spatial extent (Alkema, 2007, Wang et al., 2008, Leenders et al., 2009). These parameters are extracted from the models used. Hydrographs are useful to determine flood peaks and runoff volumes. Flood disaster management relies on knowledge and information about the hydrological behaviour of a catchment and hence flood modelling becomes an essential tool.

Flash floods are a result from excess storage and rainfall intensity exceeding infiltration capacity (Rientjes, 2004). A logical understanding of flash floods should therefore be based on analysis of extreme rainfall events that trigger them for sound hydrological modelling. The essence of modelling floods is to enhance forecasting that allows for effective prediction hence communication to mitigate impending or progressing flood hazard. (Kelsch, 2001, Drobot and Parker, 2007, Rientjes, 2004). The need for effective monitoring and for flood warning lead time enhancement to communicate imminent hazard and disasters therefore cannot be over-emphasised.

An elaborated schematic flow diagram of catchment scale rainfall-runoff relationship was categorized into three; namely atmosphere, land surface and subsurface processes (Rientjes, 2004). Atmospheric processes include precipitation as input as well as interception, canopy evaporation, transpiration and soil evaporation as losses. The rain water reaching the surface either infiltrates or becomes overland flow forming streams and eventually into channels to effectively become catchment runoff. However, still losses through evaporation at this stage occur on streams and channels. Exfoliation adds water into the rills and streams from the subsurface processes drawing water from ground water. The subsurface processes constitute those processes supplying water from the surface that include infiltration and percolation recharging ground water. On the other hand, capillary action, exfoliation abstract water from the ground bringing it vertically upwards into higher soil zones to add to runoff processes. For flash floods, the surfaces are more important as the response of the catchment as runoff is quick. Although atmospheric and subsurface processes also occur, their rate is much lower than the rainfall intensity that exceeds the losses functions in the catchment under favourable conditions for flash floods to occur. On a slope, the rainfall-runoff processes are shown on Figure 2.1. Processes in dashed line box are crucial for flash floods study.

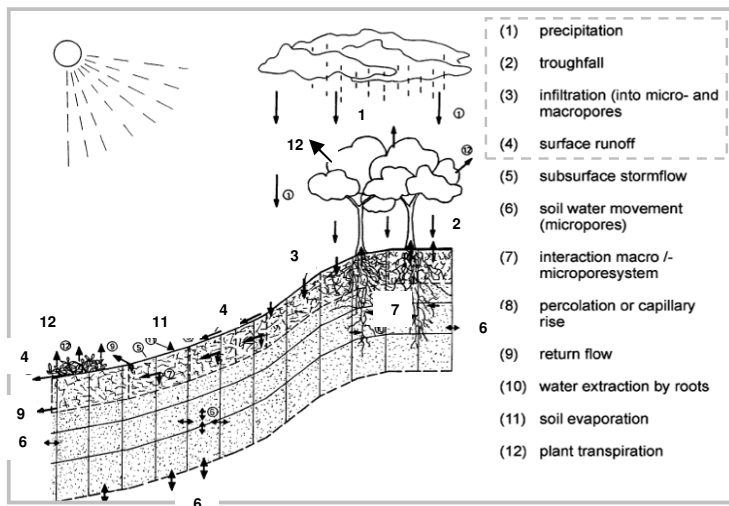


Figure 2.1: Rainfall-runoff processes.

Source: Bronstert and Bardossy (2003)

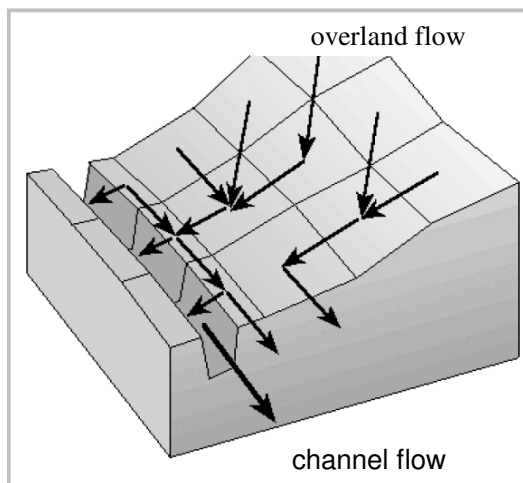
Runoff is defined as the movement of water in the streams of different sizes under gravitational influence. Runoff also termed discharge or catchment yield is measured as

volume per unit time (m^3/s^1) (Jetten, 2002). It is a function of physiographic, geologic and meteorologic catchment conditions (Rientjes, 2004). Many processes influence runoff with input in

form of rainfall, snowmelt and ground water discharge besides anthropogenic processes such as dam-break and pipe-burst among many processes. When discharge is huge discharge often overflows the banks of the channel to become a flood. The resulting flood is determined by several different factors including rainfall characteristics as discussed below.

2.2. Runoff generation processes

Runoff is generated by precipitation to become concentrated flow in stream channels and valleys. The mechanisms of runoff generation include saturation overland flow and hortonian overland flow (Rientjes, 2004). When the soil is already saturated, severe storm is likely to lead to runoff generation while hortonian overland flow process is centred on the relationship between rainfall intensity versus



infiltration capacity. This implies that, runoff is generated when rainfall intensity exceeds infiltration capacity. Aggregated subsurface storm flow (perched subsurface flow), macro pore flow and rapid ground water flow are the other runoff generation mechanisms (Rientjes, 2004). In a nutshell, high intensity rainfall causing a quick runoff response may result in a flash flood. Figure 2.2 illustrates the flow being directed to the channel from the upland surface (Jetten, 2002).

Figure 2.2: Runoff generation process.
(Source: Jetten (2002)).

2.3. Factors controlling runoff

The measure of the response of a catchment to runoff is better portrayed as lag, that is, time from centroid of rainfall to peak runoff to the peak time of the hydrograph (Houghton-Carr, 1999). This delay factor is determined by the catchment shape and size, vegetation cover, topography, soil type and subsurface factors (soil layers and rock layers) as pointed out by Abulohom et al (2001). Houghton-Carr (1999) argued that the quality and definition of rainfall-runoff relationship is related to scale (spatial and temporal). According to Dunne (Rientjes, 2004) concave hill slopes, thin soils and wide valley bottoms are important in the generation of overland flow. Steep-slopes are more likely to influence fast flow of water from the area and thus quick response of the catchment by runoff with reduced residence time for the water to infiltrate, except where there are some depressions to store the water. When a catchment responds quickly to a runoff generating process such as high intensity rainfall, a flash flood is generated.

Soil moisture as determined by several factors is important in runoff generation. Soil plays an important loss function in runoff generation. Soil texture, structure, pore size and distribution are important in determining soil physical properties including saturated hydraulic conductivity, porosity and initial soil moisture. These physical properties are important as they determine the quantity of surface water available for runoff in relation to infiltration. High infiltration in combination with deeper soil reduces the amount of water available at the surface leading to less runoff (Dhar and Nandargi, 2003). Infiltration is determined by many factors that include vegetation, rainfall characteristics (duration, intensity and type), soil physical properties, texture, organic matter, structure, pore size and distribution and soil moisture.

Storage is important in runoff generation as a function of topography, land cover and surface configuration. Where soils are deeper, highly porous and permeable, the chances of overland flow are reduced (SOBEK Online Help). Depressions were noted to have significant storage effects on watershed surface that important for water retention (Abedini et al., 2006). Excess surface storage and higher rate of precipitation to infiltration leads to the generation of surface overland flow that moves downslope under the influence of gravity through the hortonian overland flow (unsaturated overland flow) process. When soil is already saturated, severe precipitation is most likely to be available for runoff as the soil is already saturated and the ponds and depressions may be filled by the previous storms resulting in saturated overland flow (Beven, 1997). In flash floods, surface processes and top layer of the soil is the focus of the surface runoff and flash floods that are a quick response of the catchment. Baseflow contribution is often assumed to be less important as the runoff is a quick response to severe precipitation, dam-break or other influential factors.

Vegetation significantly influences the amount of runoff generation. It serves a storage function through interception thereby reducing the rainfall amount reaching ground to become runoff. Throughfall, stem-flow, leaf and stem drainage constitute the portion of rainfall that eventually reach the ground while intercepted rainfall evaporates as Rientjes (2004) outlined. Dense vegetation cover with the correct leaf distribution and orientation reduces the rainfall reaching the surface as throughfall by increased interception. Such an effect increase, loss (storage) and thus reduces the potential amount of runoff to be generated. The reverse is true for less or absence of vegetation. It follows that less vegetation is favourable to flash floods due to significant reductions in interception loss.

Land management and land use practices are important in determining the land cover and its associated influences and soil conditions important in the runoff generation process. Plantations and croplands influence runoff differently. Tilling the land during the growing season promotes infiltration by loosening soil hence reduces runoff. Terracing reduces the slope gradient, promotes

ponding and surface storage thereby reducing the amount of water available for runoff. Artificial channels such as canals, compacted paths and surfaced roads and pavements are important in the generation of runoff because they reduce infiltration while acting as channels.

Beven and Binley (1992) concluded that water table information was of little use after they examined its effect by calibrating a physically-based rainfall-runoff model. In that view, water table data can be dispensable since the behaviour and characteristics of flash floods as a quick response to input (rainfall). Baseflow is a much slower process than intense rainfall event that would trigger flash floods (Beven, 1997). Hortonian overland flow is an important process to explain rain-driven flash floods.

2.4. Hydrographs

The shape of the catchment and the drainage density determine the shape of the hydrograph (Rientjes, 2004). Additional factors include soil, geology and human influences such as dams and channel modifications. The shape of the hydrograph is important to understand the catchment response (runoff) to the respective input (rainfall) that is the rainfall-runoff relationship (Rientjes, 2004). A narrow and sharp peak hydrograph is associated with a roundish catchment with streams converging almost at the same place due to the same time of concentration to discharge huge volume at once when the a high intensity storm is experienced. Such hydrographs are good signals of flash flood event. A narrow, longitudinal catchment with tributaries joining at different location on the main river tend to produce a subdued but long duration peak and in a small catchment, this is less likely to cause flooding. The area under the curve denotes the total volume of the catchment.

2.5. Classification of floods

Dhar and Nandargi (2003) classified floods by their respective causes.

- **Flash floods:** single event floods (2-3 days) occurring in hilly terrain characterised by a sudden rising of the water levels in the river channels.
- **Seasonal floods:** occur during a particular season usually rain season.
- **Storm surges/tidal waves:** occur at the coast or estuarine.
- **Glacier melting:** occur due to melt waters.

Flash floods can further be subdivided into natural and artificial (Lin, 1999 in Bashir, 2009). The latter includes those flash floods caused by structural failures such as dam-break resulting from storms occurring with a magnitude over and above the design limits on the structure or because of a failure in dam construction while their kinetic energy is great and transport capacity is strong.

2.6. Factors influencing flash floods

Flash floods are caused by severe rainfalls as a result of typhoon or frontal system (Kinosita, 1983). Low infiltration, less interception and less surface storage or breakage of such stores are favourable

factors for flash floods as well as high drainage density, and surface compaction that reduces infiltration due to human activities. The storms of high intensity with adequate amount of rainfall triggers flash floods in conjunction with other factors including soil moisture, land cover, surface condition. High-intensity rainfall promotes hortonian overland flow that may result in flash floods. Channel geometry (shallow and narrow rivers are easily flooded) are also important.

Dhar and Nandargi (2003) highlighted that flash floods are usually a result of short duration high intensity violent storms. A study of 61 flash flood events by Maddox et al (1980) revealed that rains of 2-3cm may produce flash floods if experienced over a very small rugged drainage basin were most of the precipitation will run off rapidly. Flash floods are unique hazards associated with severe rainfall, intensive runoff development with mudflows, soil erosion and landslides with a short warning time (Kelsch, 2001). The influence of monsoons storms to cause floods in Asia, India and other regions has been widely documented. For instance, in South East and East Asia, the monsoon and typhoon driven low pressure systems cause severe rainfall leading to flooding (Kinosita, 1983) as well as in India (Dhar and Nandargi, 2003).

Bashir (2009) outlined causes of flash floods including highly localized rainfall events (thunderstorms). These causes include storms, snowmelt, natural events (collapse of a natural embankment), failure of a flood defense infrastructure, raised groundwater levels (exacerbated by saturated soil prior to large storm), inadequate urban drainage (blocked drainage network). For coastal and estuarial flooding, tidal surges or a dyke collapse induced by a wave overtopping are important processes, (Imamura and To, 1997). Kelsch (2001) highlighted that rainfall intensity is important in short duration storms triggering flash floods in small fast responding catchments making flash flood forecasting more complex than that of excessive rainfall.

2.7. Characteristics of flash floods

Flash floods occur spontaneously reaching full peak in only a few minutes up to a few hours thereby having a distinct sharp peak hydrograph (Bashir, 2009). The disaster management implication is the little or no warning time (op cit) under such circumstances. Smith and Ward (1998) noted that their rising and falling limbs are very steep with an almost equal duration. Flash floods are short-lived and destructive. The specific peak discharge of flash floods is greater than 10 and can reach a value of $100\text{m}^3/\text{s}/\text{km}^2$ (Bashir, 2009). They are extremely dangerous because of their sudden nature with high flow velocity and hence high impulse defined as a product of maximum flow depth and maximum velocity (Alkema, 2007) which helps determine areas of higher vulnerability.

Flash flood waters move very fast transporting boulders, upsetting the environment, destroying infrastructure and increase the potential for other hazards such as landslides and mudslides and may

reach between 3 to 6m height and loaded with debris (Bashir, 2009). Furthermore, while the flash floods peak discharges are much higher than for normal floods, the total hydrograph volumes of flash floods are quite small making flash flood volume not necessarily important (Bashir, 2009). An understanding of the flash floods characteristics help us to be able to predict and forecast them.

2.8. Flash flood prediction and forecasting

The prediction and forecasting of flash floods is important for decision making in disaster management initiatives. In Vietnam, different types of floods and warning systems formed the core strategy for International Decade of Natural Disaster Reduction (Imamura and To, 1997). Flash floods pose a big challenge facing humanity and are rated amongst the deadliest and dearest of all natural disasters in the world (Bashir, 2009). The cause of difficulty of prediction lies in the fact that uncertainties are inherent in modelling. The common uncertainties highlighted in literature include deterministic forcing of data, measurement errors, imperfect model structure, parameter values (calibration) (Wagener et al., 2003, Moradkhani and Sorooshian, 2009) and forecasting of flash floods is an extremely difficult and unreliable issue (Hall, 1981 and Lin, 1999 in Bashir, 2009). However, the key feature of flash flood forecasting is to identify quickly when the forecasted flood is above a certain threshold rather than the exact peak discharge and time of occurrence, which means it is not necessary to use complex models. Norbiato et al (2008) evaluated a threshold-based flash flood warning method using climatic (rainfall depth and duration) and physiographic conditions to conclude that the likelihood of a flash flood was high when forecasted rain depth exceeds the flash flood guidance threshold. The use of threshold rainfall is therefore important in flash flood studies. Threshold runoff has been defined as the amount of rainfall excess of a given duration necessary to cause flooding on small streams (Bashir, 2009).

2.9. Modelling

Modelling plays a pivotal role in flash flood prediction by way of enhancing knowledge and understanding Moradkhani and Sorooshian (2009). They (flash floods) have high destructive power combined with incredible speed, (making them sudden events) and unpredictable (Bashir, 2009). Modelling of rainfall runoff in flash flood studies has gained impetus over the years due to an increase in the effects of these hazards especially with respect to real time forecasting (Kelsch, 2001).

Modelling requires several considerations have to be addressed. While there are many models they differ essential in the structure and treatment of the different parameters of the hydrological processes as well as the assumptions they hold. Abulohom et al (2001) highlighted that there is no universal model and as such the data available, type of hydrologic quantity to be modelled, scale of the operation, accuracy required, computing facilities and economic considerations are important

considerations. Examples include, Pitman model (1973) with 12 parameters, modified by Hughes (1995) for arid and semi-arid areas and also Vandewiele and Win (1998) developed 11 parameters which differed only in formulation with eight using precipitation and evapo-transpiration while three use only precipitation as input (Abulohom et al, 2001). The crux is how the parameters are treated hence the modeller has to choose the best model which treats the loss and routing functions in the best way and optimises other parameters depending on the modelling factors. The assumptions of each model also are an important consideration in runoff and flash flood modelling. More importantly, the rainfall-runoff modelling considers runoff generation and routing functions (Abulohom et al, 2001). With the correct parameter optimisation, calibration and validation, modelling is an important tool to understand the catchment behaviour in the rainfall-runoff relationship and flash floods.

As exemplified by Wang, et al (2008) in rainfall-runoff modelling of storm events in Taiwan using regional formulae, three important features of a hydrograph include time to peak, peak flow and total runoff/discharge were useful in the prediction of floods. These characteristics are crucial in management of hazards as they have influence on both hazard effect and management initiatives such as to simulate flood hydrographs and peak that area as a result of rainfall in a catchment based on characteristics of the storm and catchment.

The use of physical based models in this regard is central as such models incorporate the catchment characteristics and tries to get into the individual processes that the 'black-box' models do not reveal. Wang et al (2008) have demonstrated the possibility to calibrate model parameters through the use of important storm event features without stream-flow data which is characteristics of most ungauged stations. However it is noted that in their study rainfall events from 32 to 162 hours were used which is not the case in flash floods triggered by short duration storm events. Integrating physical models with statistical regression analysis of three important hydrograph features (regional analysis of hydrograph features, storm event rainfall-runoff model and fuzzy multi-objective function) was noted to be important in the calibrate storm event rainfall-runoff models (Wang et al, 2008).

2.9.1. Modelling approaches

Early models tended to be conceptual bucket models that could not be justified by physical argument and theory (Ewen et al., 2006). These models do not have direct physical interpretation (Wagener et al, 2003). Beven (1997) further argued that at catchment and higher levels, other factors than pure physical soil characteristic heterogeneity assume more importance in the governing of hydrological responses. Physical based models are therefore, better suited to much smaller scale areas where the soil physical characteristics are more characterized than on a much larger area. The issue of spatial variability of input rates such as rainfall and effects of geology, topography, control of subsurface flow among others is important, as Beven (1997) further argued. Physical based models tend to be

data intensive due to their attempt to explain the processes between the input and output with many parameters and processes. Yet each of the intermediate processes are complex as well in themselves (Chiew et al., 1993). Data is often a challenge for such approaches. A third approach in rainfall-runoff modelling, conceptual models, involves conceptualising a catchment as constituting several interconnected storages. This is a description of the movement of water with mathematical functions into, between, and out of these storages. The catchment physical processes are often attempted but also include 'black box' approaches, with empirical equations and 'effective' parameters used to describe the processes. The conceptual models could therefore be commented to be a blend of the 'black-' and the 'white-box' models thereby positioning them in between the two, hence are 'gray box' models.

2.9.1.1. 1D Runoff modelling

Both rainfall-runoff and flood modelling can either be done using a lumped or distributed model or intermediate between the two, semi-distributed. Distributed model caters for each smallest individual unit for example modelling that takes care of individual pixel (raster-based) in a catchment with thousands or millions of raster cells. A lumped model considers the whole catchment as a set of sub-homogeneous units. Modelling also varies by approach for instance stochastic (probability distribution of the variables in the hydrological system) versus deterministic (physical processes simulated). In rainfall runoff modelling, available models include LISEM (Jetten, 2002), Pitman (Abuholom et al, 2001), Topmodel (Beven, 1997) among others.

In distributed models, pixel size is important. However the unit of measurement, for instance, hill slope processes, requires a pixel size that caters for the smallest slope unit (Beven, 1997). In rainfall-runoff modelling, temporal data with high resolution is also important especially as time series of discharge and rainfall in runoff modelling. Other important modelling issues include parameter optimisation, calibration, sensitivity analysis and validation. Calibration and validation require observed data to improve the model performance. One important challenge though is modelling dike breaks (also known as dam breaches) to understand the effect in terms of flood generation and propagation.

Models used to estimate runoff (output) from rainfall (input) are often classified into either 'black box' or 'process models'. The former modelling approach uses empirical equations for instance simple mathematical equations and time series relate runoff and rainfall which are the only two with physical meaningful (Chiew et al., 1993). The same applies to flood modelling. On the other hand, process models attempt to simulate the hydrological processes in a catchment in much detail. The approach uses many partial differential equations to govern various physical processes and equations of

continuity for surface and soil water flow according to Chiew (1993). Physically-based models are classified as white-box models due to their attempt to detail the processes between inputs and outputs.

2.9.1.2. 2D Flood modelling

Physically based hydrodynamic models apply Saint Venant's equations to quantify the water as a function of topography, as Alkema (2007) outlined. Flood modelling incorporates rainfall-runoff, or discharge data largely the hydraulic models such as HECRAS, HEC-HMS, Sobek, MIKE II, MIKE 21, LISFLOOD, The 2D hydraulic models simulate the flow in both horizontal directions of the plane. These models are based on the principle of conservation of mass, momentum and energy. This means that there is a mass balance and momentum balance check at every calculating point where the water is in terms of whether it is in the channel, overland or stored on the surface depressions.

2.10. Conclusion

Rainfall-runoff modelling has been widely applied in many different catchments. While the approaches have differed significantly based on model structure, assumptions, calibration, validation and evaluation, the scale of simulation has often been on a coarser resolution in both temporal and spatial scales. This does not seem to adequately address the flash flood problem since the event can occur just a life time of a few minutes or hours. Beven (1997) highlighted that the pixel size, hence spatial resolution, is dictated by the smallest unit that the model tries to simulate. The same also applies to the temporal resolution. This implies that flash floods which occur in a few minutes to several hours require also a time series of the same resolution for both rainfall and discharge. The application of coarser temporal resolution under flash floods circumstances is therefore unjustifiable. While many studies have assessed spatial resolution and its effects, the temporal resolution is still gray area for assessment. The spatial and temporal resolutions of equal magnitude to the flood event under study is ideal. The sensitivity of flash floods as a result of topographic modification by humans is a critical subject for assessment.

3. Methodology and data

3.1. Introduction

Storms are important for initiating flash floods as literature review (Chapter 2) demonstrated. A tool capable to model this problem at catchment scale was therefore necessary hence the applicability of LISEM. However, due to the complex terrain in the rice paddies, a suitable flood propagation model, SOBEK was important to understand the flood propagation and extent. A stepwise approach combining 1D and 2D models proposed by Alkema (2004) was found appropriate for this study. Modelling was an appropriate tool to answer the research questions posed in Chapter 1 pertaining to the role of land use and soil physical properties in influencing both runoff and flash floods. However, modelling data-needs for catchment runoff yield and flash flood propagation were met through the process outline below. Specific data-needs were met through primary and secondary data collection processes as outlined on Section 3.4.

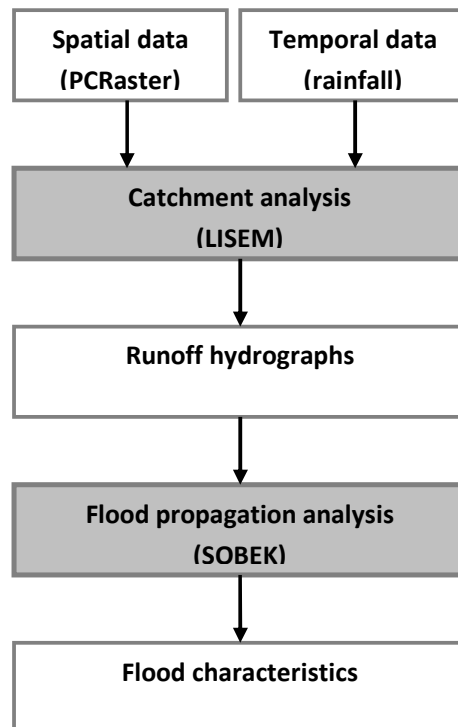


Figure 3.1: Study methodology

3.2. Data requirements of LISEM and SOBEK

3.2.1. LISEM data requirements

The model structure of LISEM outlining important model parameters is shown on Figure 3.2.

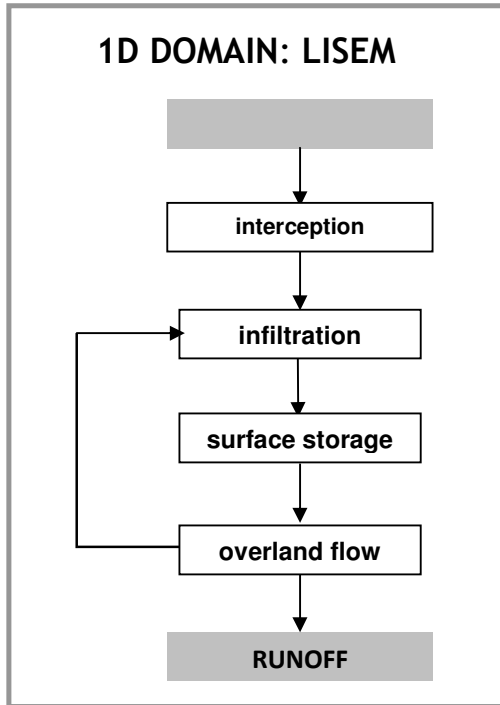


Figure 3.2 shows the rainfall-runoff module for LISEM with the soil erosion option switched off. LISEM is a data intensive model, requiring at least 24 maps for the runoff simulation. However, using a PCRaster script (Appendix 3.1) that derived parameter maps from five basic maps (DEM, land use, soil, channel and road) in conjunction with a table of soil physical properties (measured using field samples), the database for LISEM was created. The data requirements for LISEM are listed on Table 3.1 and some of the maps are on Appendix 3.2.

Figure 3.2: LISEM rainfall-runoff module

(Source: Jetten, 2002)

Table 3.1: Input parameters for LISEM rainfall-runoff modelling.

PARAMETER	NAME	METHOD	RANGE
Catchment data			
Local drain direction	LDD.map	DEM derivative	1-9
Catchment boundary	AREA.map	DEM derivative	1
Rain-gauge area	ID.map	Field observations	1-n
Slope gradient	GRAD.map	DEM derivative	>0 & <=1
Outlets	OUTLET.map	DEM derivative	1
Outpoints	OUTPOINTS.map	DEM derivative	1-n
Rainfall data	ASCII table	From Nguyen	1-n
Vegetation			
Leaf area index	LAI.map	From PER.map	0-12
Vegetation cover fraction	PER.map	Field observations	0-1
Vegetation height	CH.map	Field observations	0-30
Soil surface			
Manning's n	N.map	From literature	0.001-10
Random roughness	RR.map	From literature	0.05-20
Width of roads	ROADWIDT.map	From Nguyen	0-cellwidth
Hard surface	HARDSURF.map	Field observations	0 or 1
Infiltration (Green & Ampt : 1 layer)			
Saturated hydraulic conductivity	KSAT1.map	Field experiments	0-1000
Saturated volumetric soil moisture content	THETAS1.map	Field experiments	0-1
Initial volumetric soil moisture content	THETA11.map	Field experiments	0-1
Soil water tension at wetting front	PSI1.map	From literature	0-1000
Soil depth	SOILDEP1.map	Field observations	0-1000
Channels			
Local drain direction of channel network	LDDCHAN.map	From LDD.map	1-9
Channel gradient	CHANGRAD.map	From GRAD.map	0.0001-10 6
Manning's n for the channel	CHANMAN.map	Form literature	0.001-0.6
Width of channel	CHANWIDT.map	Field observations	0-cellwidth
Channel cross section shape	CHANSIDE.map	Field observations	0-10

LISEM has four important sub-models that are simultaneously simulated using rainfall input to give runoff output. The importance of each of the processes in the model to influence runoff was outlined in the literature review (Chapter 2). Rainfall data (input) is the storm event as a time series. Interception loss is modelled using vegetation parameters, infiltration (soil storage) loss by Green and Ampt model while surface storage is based on random roughness parameter. Overland flow is routed using the solution of the kinematic wave (Jetten, 2002) and Manning's equation. The channel parameters are useful as the runoff is directed to the outlet. Runoff (m^3/s) time series is the output which was an important input to SOBEK model.

3.2.2. SOBEK data requirements

In Sobek, each scenario is named a 'case'. SOBEK model has eight stages as represented by their respective task blocks shown on Figure 3.3 in each case. The task blocks 'Meteorological Data' and 'Import Network' were switched off while 'Settings' task was to communicate between modeller and model on time and output settings. SOBEK input data is used to characterise the network in network editor (NETTER) in the 'Schematisation' task before the simulation is initiated. A summary of SOBEK data requirements is presented on Table 3.2.

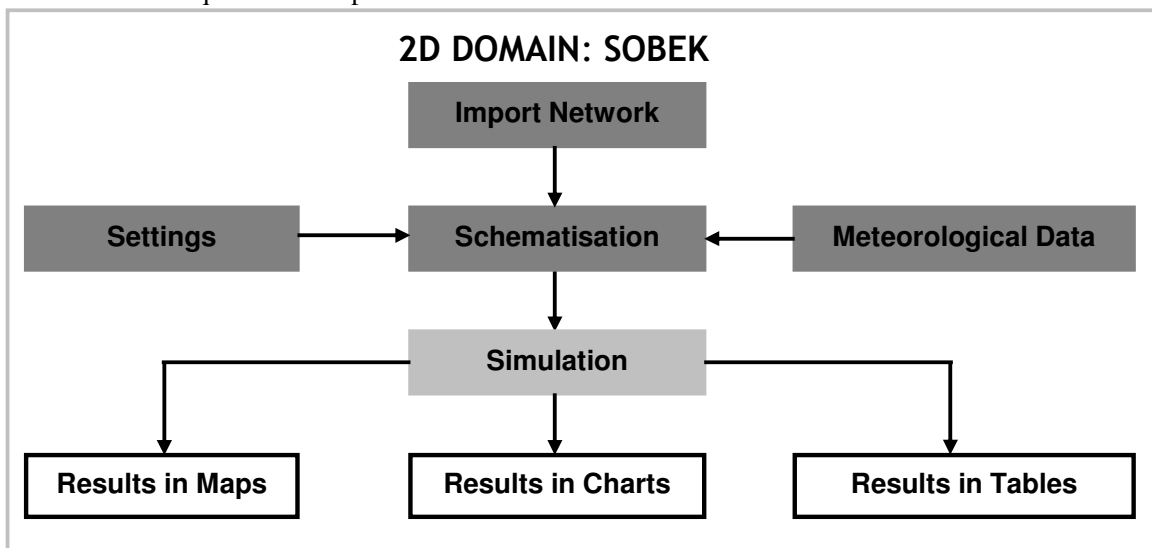


Figure 3.3: SOBEK model; pre-simulation, simulation and results blocks.

Table 3.2: Input parameters for SOBEK flood propagation modelling

PARAMETER	NAME	METHOD	format
2D spatial data			
Elevation	DEM	contour interpolation	asc
Roughness	Friction map	land use + literature	asc
1D spatial data			
River	Long profile	From image (digitising)	vector
River	Cross section	Field measurements	(numeric)
Temporal data			
discharge	Discharge table	From LISEM output	txt

3.3. Pre-field work Inventory

From the detailed data requirements outlined in Section 3.2, the inventory of data needs was created on basis of available and needed data as shown on table 3.3.

Table 3.3: Inventory of data

AVAILABLE:	resolution	type	source	UNAVAILABLE DATA:
Elevation	10m	DEM, contour	Nguyen	River cross sections
Spot (2004/12/14)	10m	Image (3 bands)		Discharge
Topographic map	-	map		Rice field features
Quickbird (2008/05/12)	0.5m	Image (4 bands)		Dikes and break evidence.
Google (2006/08/02)	0.5m	Image 3 (bands)		Water bodies geometry
Worldview (2008/05/12)	0.5m	Image (<i>pan</i>)		Land uses (present)
Land use	10m	(classified image)		Soil physical properties
Soil texture	10m			Historic floods data
roads	10m			Buildings elevation
rainfall	(see * below)	Excel tables	various	

**Rainfall data resolution: daily (1960-2008), hourly (2007 -2009), 10minutes (2008-2009)*

In order to meet the data requirements for the two models' as outlined in section 3.2, a field campaign to collect unavailable data was undertaken from the 11th of September through the 2nd of October 2009 in the study area. The data collection process is outlined in the following section.

3.4. Field work data collection

The data collection included land use observations, soil sampling, measurement of discharge, channel geometry, ponds and rice field features (ridges, dikes, terraces) and observations of soil depth at the roads cuts. Interviews about past floods were held in the area. The spatial data was captured using a Garmin E-Trex 12 channel. The process is as outlined below.

3.4.1. Mapping land use

Land use types and land cover characteristics were observed and recorded at every point where a soil sample was collected. Vegetation type, height, percentage cover and age of the vegetation.

3.4.2. Sampling strategy

A spatially stratified random sampling was applied in collecting soil samples during fieldwork. The sampling was based on the lithology and land use as tabulated on Table 3.4.

Table 3.4: Sampling strategy for soil samples.

LAND USE	AREA (km ²)	%	TARGETED
Bare soil	0.1	01	01
Grass and shrubs	0.7	05	03
Mature forest	7.1	49	30
Rice field	1.3	09	05
Mixed trees	4.6	32	19
Other	0.5	04	02
Total	14.3	100	60

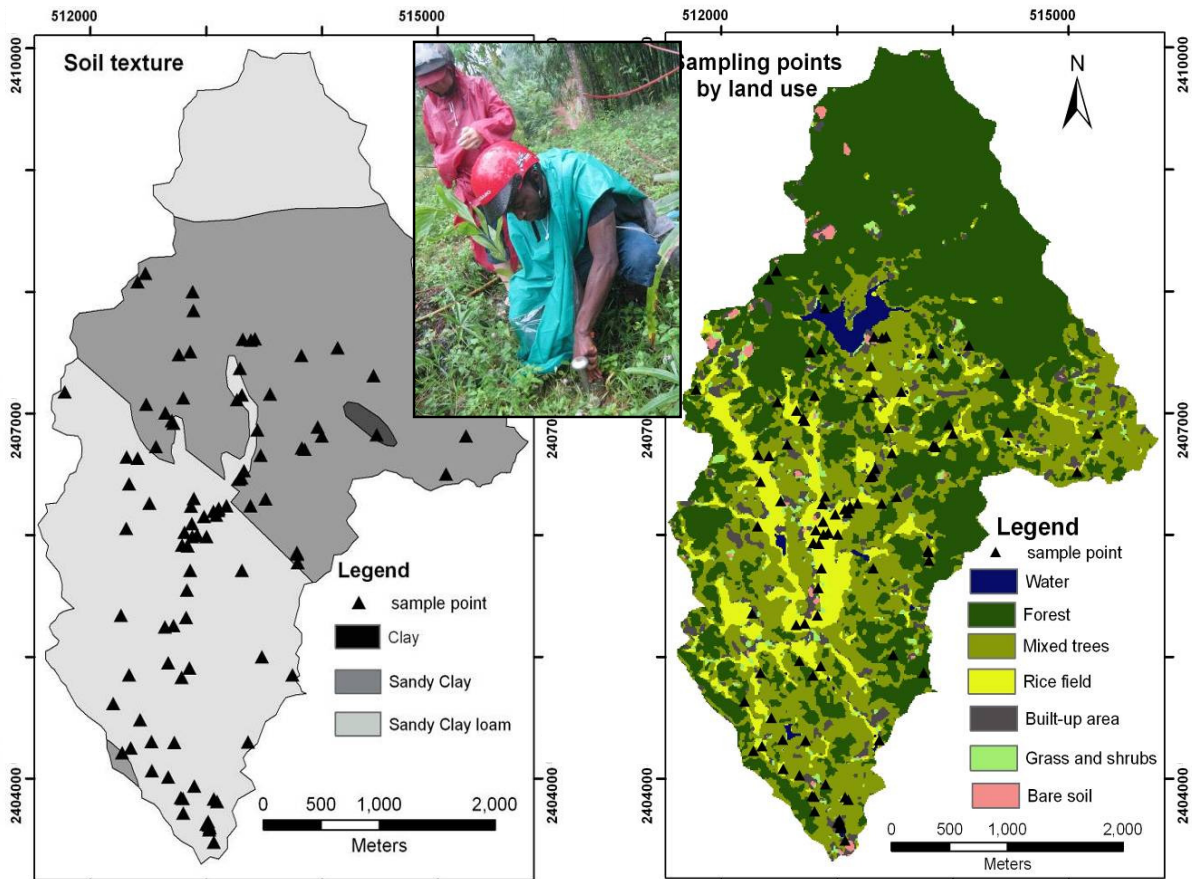


Figure 3.4: Spatial distribution of soil samples by soil texture.

Figure 3.5: Spatial distribution of soil samples by land use . (The insert is a picture of the sample collection process)

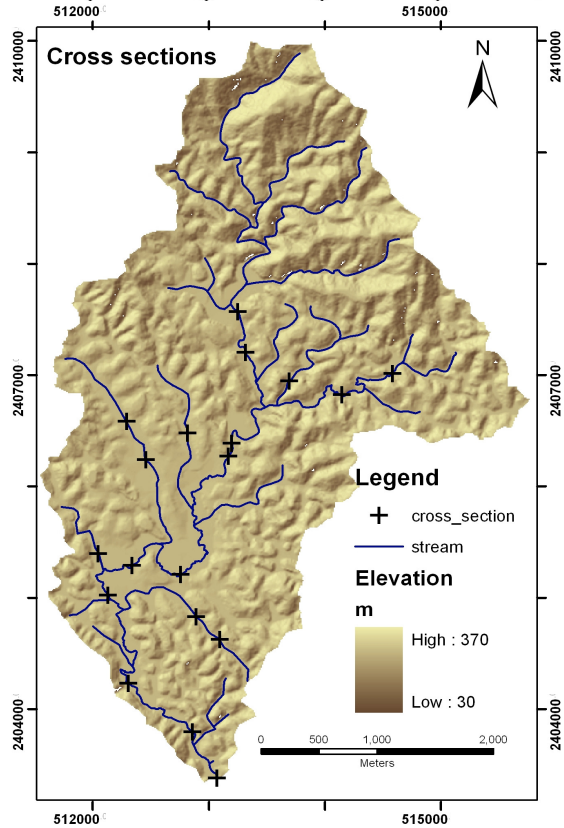


Figure 3.6: Points of cross section and discharge measurement.

The number of samples per unit land use type was determined by the proportion of the area. A total of 84 were collected instead of the targeted 60. The northern forest was inaccessible due to impenetrable density of vegetation. Convenience sampling was done in the rice fields due to inundated soil and eventually more samples were collected in the land use. More samples were collected in the mixed tree plantations, tea and rice fields than in other smaller and scarcer land uses.

3.4.2.1. Soil Sampling

Undisturbed soil samples were collected using the above mentioned sampling strategy. A 50mm diameter core sampling ring was inserted into the holder, hammered into the top soil layer as shown on Figure 3.4 (insert). It was then dug out using a spade and sliced at the bottom of the ring with the sample in an upside down position to first to ensure that the soil lump remained intact. Plastic caps were inserted after slicing the edges. The same procedure as outlined by Panchansri (2007) was followed.

Sixty samples were collected and analysed for saturated hydraulic conductivity (Ksat) during the field campaign in Vietnam and an additional 24 were collected and analysed in ITC laboratory for Ksat, porosity and initial soil moisture content. Additionally, 17 analysed results for the three soil parameters were provided by Nguyen. The location of selected soil sampling points in soil texture and land use is shown on Figure. 3.4 and 3.5 respectively.

3.4.3. Cross sections

Cross sections were measured at certain points on the main channel and other tributaries in the catchment. Photographs of the cross section measurement are as shown on Appendix 3.3. Two lines, one tightly fixed and the other with a sliding notch, were stretched across the channel to allow the measurement of the depth across the tight rope. Cross section was measured from left bank facing down slope, the depths of the 50cm interval. A second detailed cross section at 1m interval was done at the outlet bridge. Eight intermediate cross sections between the bridge and the spillway in addition to nine on other tributaries were measured as shown on Figure 3.6.

3.4.4. Water bodies

Water bodies and their respective characteristics were mapped using GPS and digitised from the high resolution World View image. Their approximate length and width were measured or approximated and depth was inquired from the local people whenever necessary. Characteristic cracks in the walls of the ponds were observed as shown on Figure 3.7. Notes and photographs of these ponds were captured during the fieldwork exercise. A map of the water bodies in the catchment is presented on Figure 3.7a.

3.4.5. Rice paddy elements: Dikes, terraces and 'ridges'

Rice field 'ridges' and terraces dimensions (width, depth, length) in the rice fields were measured using tape measure. Figure 3.8 shows the terraces and measurement process. This was important as to determine the terrain that were used to model the landscape DEM level slices in the subsequent flood modelling so as to better represent the terrain features more accurately.



Figure 3.7: Cracks on dikes and ponds



a



b



c

Figure 3.8: View of terraces (a) and the measurement of height (b) and width (c)

3.4.6. Discharge

The measurement of flow velocity was done where cross sections were done using a current meter. Readings from the different depths were recorded and then averaged to get the average flow velocity of the discharge. However, it was noted that the flow was too shallow upstream (23cm) and at the outlet bridge, stagnant water and the blocking of the channel with bamboo made it impossible to deep the current meter to measure velocity of flow. Also due to small rain events during the measurement period, there was no noticeable flow effect on the streams.

Flow depth time series data at 10 minutes temporal resolution was calculated based on data from two 2-channel mini-diver 14 (M2.11.11.E) installed at the bridge (catchment exit) and near dam (upstream). The depth was measured using a graduated rod and tape measure lowered into the river at consistent intervals. The depths of the cross section and water in the channel were noted and sketched for discharge calculation. The depth of the flow at the upstream and downstream parts were done at the location of the two mini-divers.

The formula for calculating the water level was extracted from the mini-diver manual using the formula;

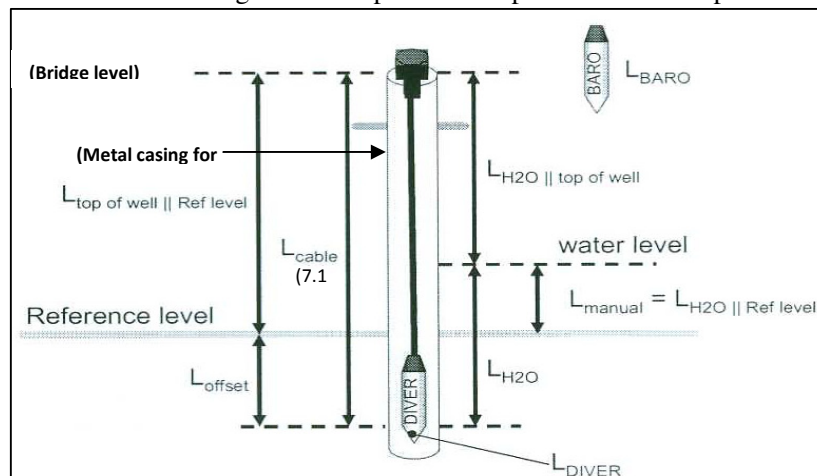
$$L_{H2O||ref\ level} = L_{top\ of\ well||Ref\ level} - L_{cable} + L_{diver} - L_{baro} \quad (3.1)$$

Each parameter of the formula is diagrammatically shown on Figure 3.11. Readings from the mini-diver were converted from pressure and temperature to water head/column using the Diver Office software.

Mini-diver at the bridge was installed in July 2009 while that on the upstream was installed during the fieldwork. The discharge depth was then calculated from the time series of the diver downstream as a calibrating parameter for the flood model since the exit boundary was depth was used in the absence of a longer time series data with any flood events experienced in the area as constrained by the short duration of installation. Interviews were also designed to complement the past extent and depth levels of the previous flood events and the indications were noted.

Figure 3.9: Factors in the calculating the water level using equation (3.1).

(Source: (Eijkelkamp, 2003) with additional annotations).



3.4.7. Interviews

Interviews with local farmers, officers at the district office and the community members concerning their experience knowledge and understanding of historic flood events was gathered using some interview questions. The 2008 flood event appeared to be more vivid in the people's minds and all reference was inherently to this event and earlier floods were no longer fresh in the minds and people were indicating some high level of having forgotten those events. A copy of the questions is as shown on Appendix 3.4. The depth relative to the local and nearby features such as bridges and other noticeable structures such as buildings were done and the indications of the people noted. This information was useful to understand the lateral spread/propagation of the flood waters as well as the depths and speed of flow. However, the effectiveness of this method of data collection was hindered by the lack of the interpreter on most cases. Furthermore the velocity of the flow was very difficult to quantify and as a result the depth and extent was considered to be important in the flood propagation in the catchment.

3.4.8. Secondary data

Rainfall data that was available for the study is outlined on Table 3.4. The graphs showing the rainfall parameters are presented on Appendix 3.5.

Table 3.5: Rainfall data for study area

Resolution	Period	number	Name of Station
daily	1960-2008	1	Yen Bai Meteorological Office
hourly	2007-2008 (Jun-Oct)	1	Yen Bai Meteorological Office
10 minutes	2009 (Jul-Dec)	2	Cuong Thinh Meteorological Office

3.5. Post field work data processing

3.5.1. Soil physical properties

Post field work involved the analysis of soil samples to determine soil physical parameters to use in LISEM. Saturated hydraulic conductivity (K_{sat}), porosity, initial moisture content and bulk density were determined as outlined below.

In the field the measurement of 60 K_{sat} samples was done using the experiment setup as shown on Figure 3.10a and b. The sample was soaked for at least 24 hours and then K_{sat} measured.

Field work Ksat experiment.

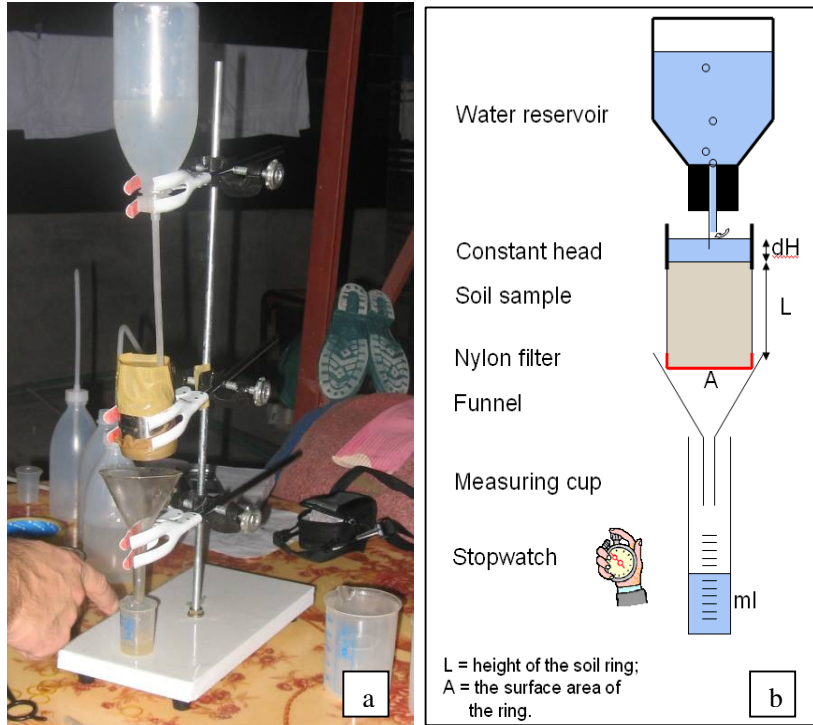


Figure 3.10: Ksat field experiment.

The formula for calculating Ksat was;

$$K_{sat} = \frac{Q}{A} \cdot [L(L + dH)] \quad (3.2)$$

Where K_{sat} is the saturated hydraulic conductivity, Q is percolation rate, A is surface area of ring, L is length of ring and dH is depth constant.

For the 24 samples analysed in the Netherlands, the laboratory permeameter (M1.09.02.E) was used. The experiment was done as outlined in the operating instructions (Eijkelkamp, 2003).

Soil sample was saturated in the permeameter over at least 24 hours. Then basing on the rate of draining the measurement of Ksat was done. Fast draining soil samples were measured using a constant head method after setting the head to the minimum prescribed for the instrument (2-20mm). the head was reduced closer to minimum for fast draining samples and the readings were either based on time interval of 5 minutes or the time it took to reach every next 10ml.

After determining the rate of draining and converting the units, the formula used for the Ksat measured using the constant head was:

$$\kappa = \frac{V \cdot L}{(A \cdot t \cdot h)} \quad (3.3)$$

Where: K is Ksat (cm/d), V is volume of water flowing through sample (ml), L is length of soil sample (cm), A is cross sectional area of the sample (cm²), t time used to flow through of water volume (V) and h is water level difference inside and outside ring holder (cm). The units of the

permeameter are in ml and cm hence there was need to convert to mm units for use in the model. (Eijkelkamp, 2003).

Falling head method was used to measure Ksat for very slow draining samples that required more time just to drain a few millilitres of water. Soils with more clay content tended to drain slowly and even their soaking took more than one day. Readings were spaced after longer time spaces of about one hour and also some were left overnight. The formula for the falling head method had a different inclusion of additional variables as shown on the equation below;

$$K = \frac{a \cdot L}{A \cdot (t_2 - t_1)} \cdot \ln \frac{h_1}{h_2} + \frac{x \cdot a \cdot L}{A \cdot \sqrt{(h_1 \cdot h_2)}} \quad (3.4)$$

Where A, K, and L water level difference inside and outside ringholder are the same as above. Additional terms $t_2 - t_1$ is time between start and end of measurement, the same factors are determined for as equation 3.4, h_1 and h_2 is water level difference inside an outside of ring holder and a is cross sectional area of ring holder (Eijkelkamp, 2003).

Porosity test porosity measurement followed after the measurement of Ksat. After measurement of Ksat the soil sample was drained for a few minutes before measuring its saturated weight using a scale. The saturated weight was important to determine the saturated volumetric moisture content which is a requirement of the LISEM model. The calculation was done in two stages first to determine pore volume by subtracting weight of dry sample from saturated sample with both weights corrected for ring weight. Weight is converted to volume ($1\text{cm}^3 = 1\text{ml} = 1\text{g}$). The volumetric soil moisture was then determined calculated as;

$$\text{Pore volume (PV)} = (W_s - W_r) - (W_d - W_r) \quad (3.5)$$

Where W_s is saturated weight of sample, W_d is dry weight of sample and W_r is weight of ring

$$\text{Porosity } (\theta_s) = (\text{PV}/\text{RV}) * 100 \quad (3.6)$$

Where RV is the ring volume.

Initial soil moisture test the soil was measured as intact with the caps on the soil sample was measured from the field. After all the testing was done and the weight of the ring and plastic caps were subtracted form the weight measured initially from the field then the initial moisture content was also determined in two steps as determined as summarised by formula below;

$$\text{Field moisture volume (FMV)} = (W_f - W_r) - (W_d - W_r) \quad (3.7)$$

Where W_f is the field weight, and the other values as defined above such that the

$$\text{Initial soil moisture content } (\theta_i) = (\text{FMV}/\text{RV}) * 100 \quad (3.8)$$

The resulting soil physical properties assessed from the soil samples brought into the ITC laboratory are Ksat, porosity, field moisture content and bulk density. A summary of the statistics of measures of central tendency and dispersion for Ksat by land use and texture is presented on table 3.5 and 3.6.

Table 3.6: Ksat (mm/h) by land use class

Land use	Minimum	Maximum	Mean	Median	Standard deviation	n
Grass and shrubs	0.5	516.6	76.0	29.7	114.7	30
Rice	0.2	351.6	53.7	22.4	87.3	35
Trees	0.2	438.8	82.7	34.5	115.3	30

Table 3.6: Summary for the Ksat values

Texture	Minimum	Maximum	Mean	Median	Standard deviation	n
Clay	100.7	100.7	100.7	29.7	n/a	1
Sandy Clay	0.2	351.6	57.9	23.2	87.3	37
Sandy Clay Loam	0.2	438.8	77.2	31.0	116.3	57

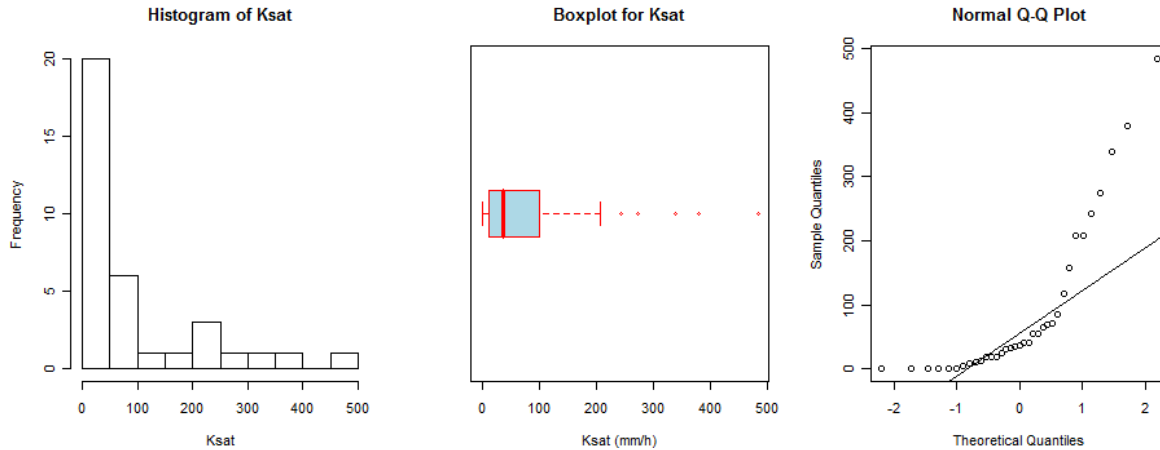


Figure 3.11: Histogram (a), boxplot (b) and quantile-quantile plot (c) for Ksat.

The three graphs Figure 3.11 confirm that the distribution of Ksat in the catchment is positively skewed. It was reasonable to consider the median value that is not influenced by extreme values, as representative of the land use category in the determination of Ksat after results of interpolation proved unsatisfactory due to the distribution of data points, instead of the mean.

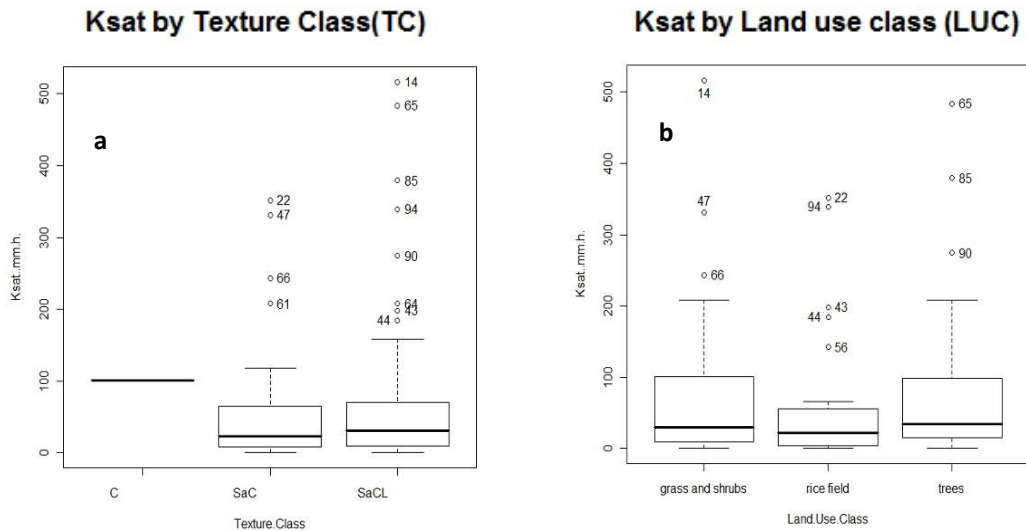


Figure 3.12: Box plots for Ksat by texture class (a) and land use class (b)

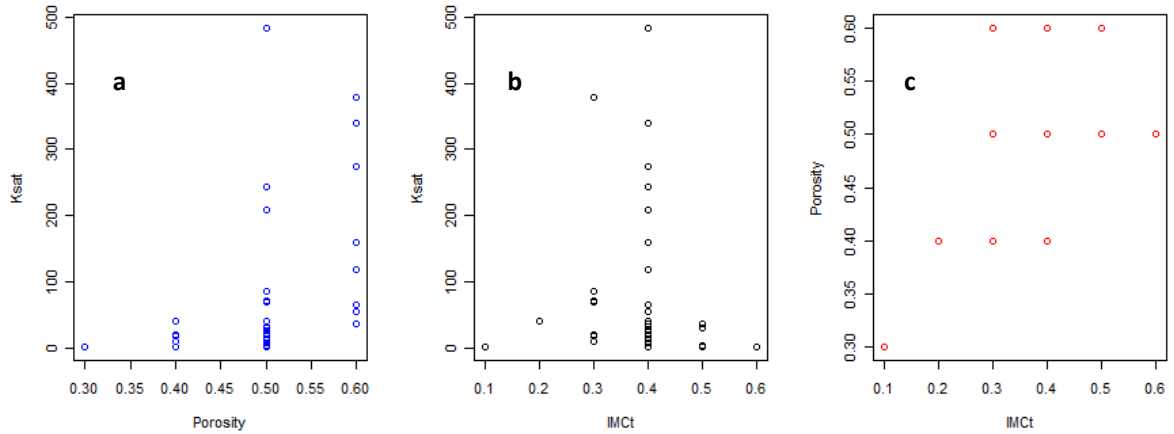


Figure 3.13: *Pairwise scatterplot of soil parameters*

The Ksat is positively skewed in both cases as also shown on Figure 3.13. The scatterplot of the Infiltration parameters are presented on Figure 3.14

This implies that neither land use nor soil type can explicitly explain the Ksat behaviour in the study area. The mean values of each land use category was considered in this case. A scatter plot of the three soil parameters is shown on Figure 3.14.

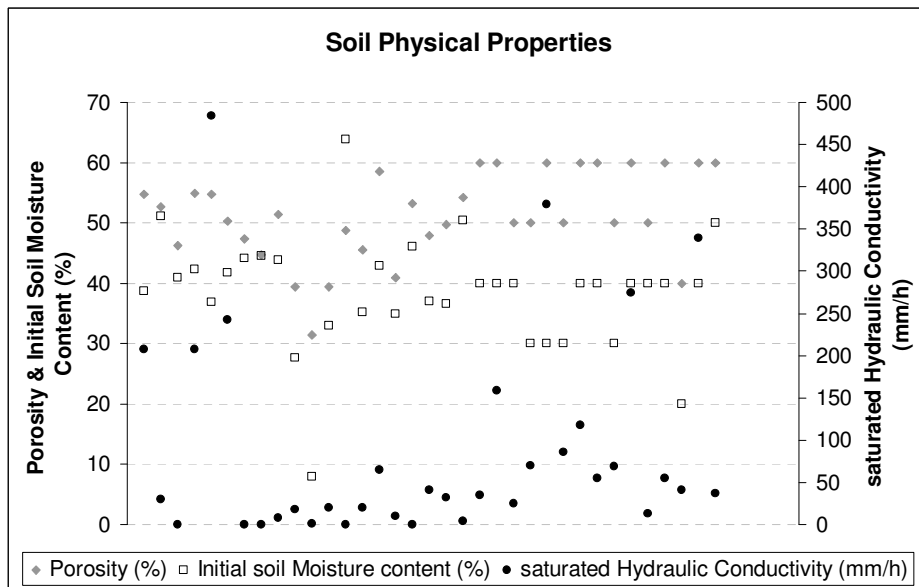


Figure 3.14: *Soil physical properties*

Figure 3.14 shows the soil physical properties in the catchment. The area has moderately high Ksat basing on the Natural Resources Conservation Service (NCRS) classification. Porosity and initial soil moisture content are moderate. The Ksat however does not reflect the theoretical values basing on texture due to higher clay content in the soils as observed in the field.

There was no distinct Ksat behaviour in the catchment based on the respective land use categories used and there is a lot of overlap in the classes. In all the identified land uses, the Ksat was right skewed.

3.5.2. DEM for LISEM and SOBEK

Two DEMs were used in LISEM, one with the whole catchment while another had rice fields masked out. The latter had 34 hydrographs that were the upstream boundary condition for SOBEK flood propagation modelling. On the other hand, SOBEK had three DEMs each for a separate scenario in the dike break, terraced slope and normal slope scenarios. The two DEMs for LISEM and one for SOBEK are presented on Figure 3.15.

3.5.3. Land use

Land use map was generated from supervised classification of SPOT image. The World view panchromatic image (date) was used to verify land uses in addition to field observations. The classification had 75% producer accuracy. The land use map is as shown on Figure 3.19. It is clearly evident that the land uses in the area are influenced by the topography. As shown on Figure 3.5a, the hilly and higher slope areas correspond to the primarily forests in Figure 3.5b. The plantations with either individual tree species or mixed plantation trees also constitute the rough and steep terrain. The trees grown include cinnamon, turpentine, bamboo, and smaller portions of bush crops including tea and cassava. Tea is an important hill crop.

The land uses are patchy due to individual household ownership. Crops grown are individually determined but there is consistency on rice growing as a staple food crop. A noticeable amount of water bodies are also evident in the area with the largest reservoir on the northern part.

3.5.4. Surface roughness

The respective land use and surface roughness also varied in spatial extents as was the cases with the DEMs on Figure 3.15 above. Surface roughness also characterised as manning's n or friction is an indication of the resistance the surfaces impose on the flowing water. It is derived from land use or land cover map. Roughness values were obtained from lookup table from literature (Alkema, 2007).

Table 3.7: The land use based manning's n values used in the flood modelling.

Land use	Manning's n
Bare soil	0.005
Built up	0.15*
Forest	0.20*
Grass and shrub	0.05
Rice	0.25*
Mixed trees	0.12
Road	0.05
Water	0.13*

(Source; adapted from Alkema, 2007 with own adjustments*)

The respective land use and roughness maps were generated based on the roughness values on Table 3.7 area shown on Figure 3.15.

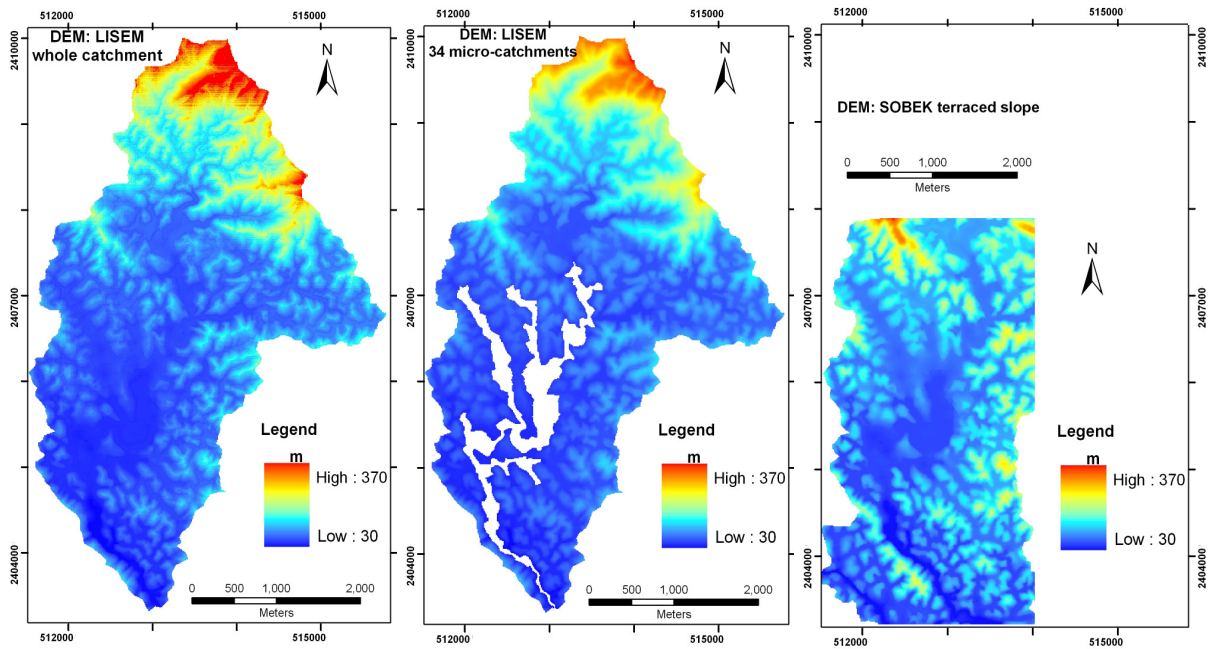


Figure 3.15: DEMs; upslope (a) and whole area (b) for LISEM and the dike-break DEM for SOBEK (c).

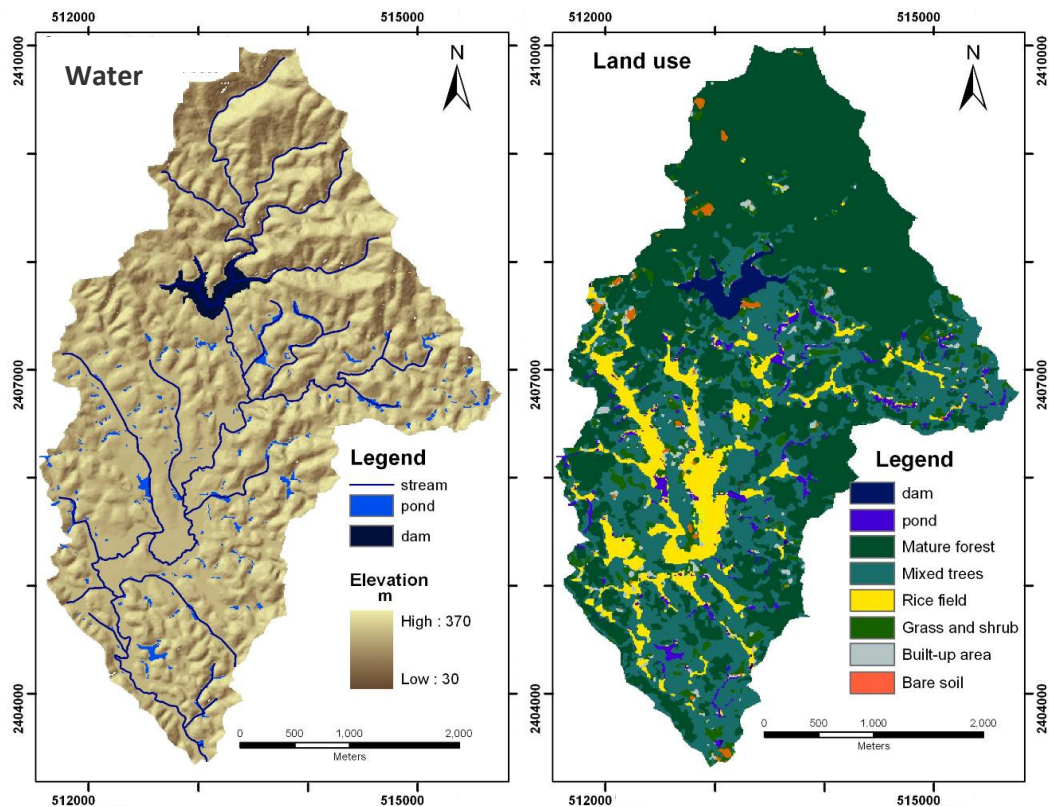


Figure 3.16: Water bodies (a) and the respective land uses (b) in the study area

The data base for the two models was therefore set to enable the modelling of the flash floods in two phases, 1D rainfall-runoff model (LISEM) and 2D flash flood propagation (SOBEK). Modelling is presented in the next chapter.

4. Modelling and Results

4.1. Introduction

The data collected and processed in Chapter 3 was then used in rainfall and flood modelling in this chapter. The rugged relief outside the rice fields were modelled for runoff using LISEM while the rice fields were simulated for flash flood propagation using SOBEK. The results of the two models are presented below.

4.2. LISEM Modelling Scenarios

All the spatial data requirements for LISEM were created in PCRaster software using a script (Appendix 3.1) that derived catchment maps from the DEM, vegetation and infiltration maps from the land use, soil depth from soil map and channels and road maps, using attributes as defined on Table 4.1. Using a script presented on Appendix 3.1, nine model parameter maps were generated from Table 4.1. PCRaster is raster software compatible with LISEM (Jetten, 2002).

Table 4.1: Measured and observed soil physical properties

	K_{sat}	θ_s	psi	θ_i	RR	n	per	ch	LAI
Water	0.01	0.1	0.1	0.001	0.01	0.13	0.01	00.01	0.1
Mature Forest	35	0.4	3.0	0.32	0.50	0.05	0.80	16.0	9.0
Rice	22	0.6	0.5	0.40	1.00	0.12	0.70	00.9	6.0
Mixed trees	35	0.5	3.0	0.40	0.90	0.04	0.75	10.0	8.0
Built-up area	33	0.3	4.0	0.25	0.30	0.03	0.60	00.1	5.0
Grass and shrubs	30	0.5	3.0	0.4	0.80	0.01	0.05	0.50	5.0
Bare soil	63	0.5	4.0	0.40	0.20	0.03	0.05	00.1	2.0

Table 4.2 used to generate the land use parameter maps namely; saturated hydraulic conductivity (K_{sat}), porosity (θ_s), suction at wetting front (psi), initial soil moisture (θ_i), random roughness (RR), manning's coefficient (n), percentage cover (per), crop height (ch) and leaf area index (LAI).

The soil physical properties (Figure 3.14) show that the saturated hydraulic conductivity is moderately high while initial soil moisture content and porosity are moderate. However there was no influence on the K_{sat} by soil texture as expected.

The LISEM modelling environment has a user interface that allows the modeller to upload input parameters, linking model to the respective maps and rainfall directories, enabling the automatic creation of a run file. Simulation time allows setting of start, end and timestep while model options enable the modeller to switch on/off runoff, erosion, snow, channels and storage. Infiltration model options allowing the choice from six of the infiltration including the Green and Ampt, the Q and D calibration options for K_{sat} and manning's n. The output options allow for specifying results directory and formats for the time series data outputs and map series.

All the spatial data was input into the model using the ‘Basic Maps’ menu bar, input output options using the Input/Output menu bar and once the loading and definitions of the data was complete, the run file was saved and then using the simulation menu bar, the modelling was initiated. The output time step was set at 10 minutes.

While the simulation is in progress, the ‘time’ and ‘water’ is shown and the summary of the simulation progress in all the defined settings including the hydrograph and sedigraph and time series of progress shown. The latest development in the model (‘Display’) allows also a visualisation of the development of nine results parameters including runoff, water height, velocity, infiltration, and soil loss related outputs (switched off in this study).

The model interface shown on Figure 4.1 and the rainfall event used in the simulation on Figure 4.2.

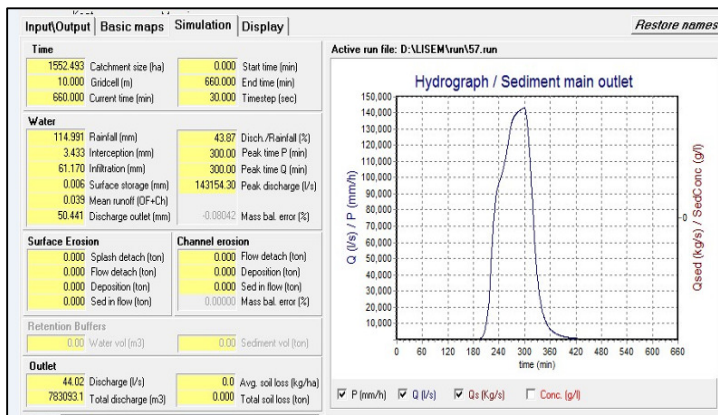


Figure 4.1: Model interface

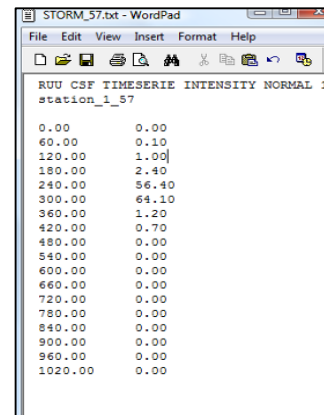


Figure 4.2: Rainfall event

4.2.1. Sub-catchments (34) scenario

Using the DEM with rice fields masked out, the simulation of the runoff was done in LISEM model. All the spatial maps were multiplied with the mask to have the same spatial coverage to allow the model simulation. Using the DEM, 34 ‘pits’ or sub-outlets defined as ‘outpoints’ in the LISEM 2.62 Beta version, (Jetten, 2010, personal communication) were created by lowering the value of the DEM so that all the surrounding water is directed to that pixel. Where there was a pit not located at the edge of the rice fields, an LDD edit in Map Edit version 1.10 (Jetten, 2010, personal communication) allowed the adjustment of the LDD to join with one that led to the rice fields or alternatively where this was not possible, calculation using a small script was used. A screen shot of the pits for the respective sub-catchments is on Appendix 4.2.

4.2.2. Whole catchment scenario.

The second scenario was simulated using the entire catchment. This was done in order to be able to cross compare the results with the SOBEK hydrograph. The spatial data covered whole catchment the rainfall used remained the same. The same outlet as the one in SOBEK was used in this scenario.

4.3. Sensitivity analysis

The sensitivity analysis was carried out for Ksat, manning's n and time step of simulation. The Ksat sensitivity analysis is as shown on Table 4.3. Literature reviewed range of the rainfall/discharge ratio; that is, the percentage of rainfall which becomes runoff or simply discharge as a fraction of rainfall Houghton-Carr (1999) was useful to check the model.

Infiltration was an important parameter in sensitivity analysis of the LISEM model as it significantly changed the value of water available for surface runoff.

Table 4.1: Results of Ksat Sensitivity to the rainfall-runoff model.

Ksat level (%)	-50	-40	-30	-20	-10	0	+50
Rainfall (mm)	115	115	115	115	115	115	115
Runoff (mm)	73	67	61	56	50	45	45
Infiltration (mm)	39	45	50	56	61	66	67
Runoff/rainfall (%)	63	58	53	49	44	39	39
Peak discharge (m ³ /s)	188	176	164	154	143	132	131
Tot volume (1000m ³)	1130	1039	951	866	783	702	694

The values resulting from the sensitivity analysis of Ksat are presented on table 4.4 show an inverse relationship between with peak discharge, total volume and runoff output. Rainfall, interception and mass balance error remained constant. However, on the positive side of Ksat, there seems to be little influence. There seems to be is a limiting threshold for the Ksat parameter. The lowering of Ksat follows after a study by Hessel et al (2003) who highlighted that field measurements of Ksat tend to be higher than those the model uses for calculations hence the emphasis on reducing Ksat.

4.4. Calibration

The model was calibrated based only on the runoff coefficient due to lack of the real flood discharge data. This was largely based on literature since the small events after the installation of the divers did not have noticeable effects. The time of the calibrated scenario was later found out to coincide with the emptying of the upstream reservoir hence results could not be reliable.

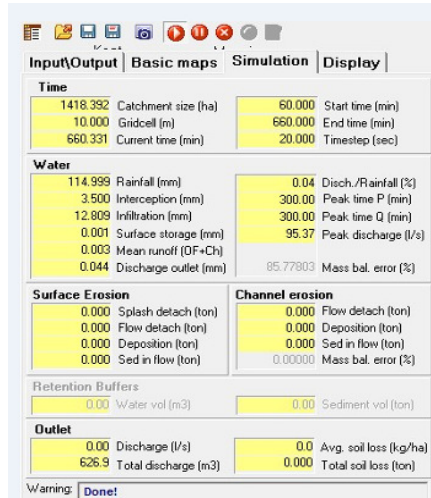
4.5. Simulation

The simulation was initiated using a time step of 20 seconds reporting every 60 timesteps, starting from 60 minutes to 660 minutes time. Figure 4.3 shows the simulation tab screen capture with the summary of the simulation and the respective hydrograph from the model. As shown on Figure 4.3, the total discharge from the catchment was slightly above 600m³ from the candidate storm event used (02/09/2007). The candidate event (Figure 4.2) was selected from 214 events on the basis of it being an isolated event, short duration and high intensity, with the informed guidance of Mr Parodi (Parodi, 2010, personal communication). All the other modelling results and settings including the catchment characteristics are also shown on this tablet. However due to the repeated model failure to cope with the same time step in the whole catchment scenario, a time step of 30 seconds was used.

4.6. LISEM results

The results from the simulation are shown on a tab that summarises the catchment and pixel size, modelling time definitions, losses and discharge amounts, outlet quantities, ratios and errors and the hydrograph which is presented on the right hand panel of the tab. A screenshot of the results interface was also presented on Figure 4.1

Figure 4.3: Simulation results as a screen shot.



Input/Output				Basic maps		Simulation		Display	
Time									
1418.392	Catchment size (ha)	60.000	Start time (min)						
10.000	Gridcell (m)	660.000	End time (min)						
660.331	Current time (min)	20.000	Timestep (sec)						
Water									
114.999	Rainfall (mm)	0.04	Disch./Rainfall (%)						
3.500	Interception (mm)	300.00	Peak time P (min)						
12.809	Infiltration (mm)	300.00	Peak time Q (min)						
0.001	Surface storage (mm)	95.37	Peak discharge (l/s)						
0.003	Mean runoff (DF+Ch)								
0.044	Discharge outlet (mm)	85.77803	Mass bal. error (%)						
Surface Erosion				Channel erosion					
0.000	Splash detach (ton)	0.000	Flow detach (ton)						
0.000	Flow detach (ton)	0.000	Deposition (ton)						
0.000	Deposition (ton)	0.000	Sed in flow (ton)						
0.000	Sed in flow (ton)	0.00000	Mass bal. error (%)						
Retention Buffers									
0.00	Water vol (m3)	0.00	Sediment vol (ton)						
Outlet									
0.00	Discharge (l/s)	0.0	Avg. soil loss (kg/ha)						
626.9	Total discharge (m3)	0.000	Total soil loss (ton)						
Warning: Done!									

4.6.1. Runoff coefficient

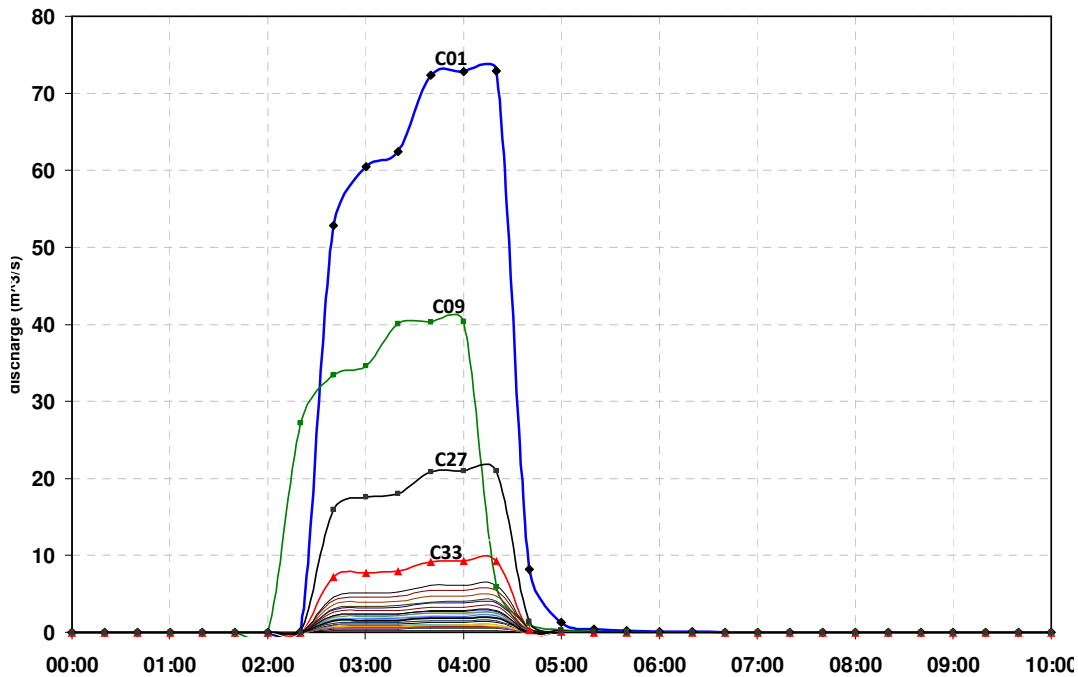
Runoff coefficient in the study was modelled between 0.4 and 0.6 which is reasonably lower than the Tone River in

Japan case study that had 200mm rainfall depth in a predominantly forest and rice land use (Kinosita, 1983) that ranged from 0.6 to 0.8. It is worthy noting that the referred study had a rainfall depth of 200mm as compared to the one used in the study which was 120mm. However in the same study Kinosita (1983) also revealed a 0.2 to 0.3 runoff coefficient for Pampanga River, with also similar rainfall and land use conditions in Philippines, thereby highlighting an important fact that runoff coefficient differs from one catchment to another. LISEM results also concur with Kinosita (1983) study that revealed the effect of agricultural developments including swamp reclamation, embankments and sophisticated drainage systems in inducing an increase in the runoff coefficient while decreasing the time of concentration. This was also the case with terracing prediction. The levelling of valley floors by terraces, positively influence on the runoff coefficient.

4.6.2. Sub-catchment hydrographs

Four outstanding contributors to the discharge are catchments C01, C09, C27 and C33 respectively, with the largest area coverage as shown on Figure 4.4.

The catchment shows a hydrograph responding in a similar fashion to a rainfall event. The shapes of the hydrographs reveal a rapidly rising discharge upon a sudden rise of the rainfall intensity with one catchment (coded C09) responding 30 minutes earlier than the others. The implication of such a runoff response is a flash flood hazard, especially in the valley bottoms. Sub-catchment C09 is located on the north eastern part of the catchment. As soon as the rainfall intensity sharply rises from 2.5 mm/h to 56.4mm/h, the sub-catchments respond immediately only half an hour after the high intensity rainfall begun. The entire catchment is very fast responding to high intensity storm events as the rainfall intensity exceeds the infiltration capacity as highlighted in several studies (Giannoni et al.,



2000, Bronstert and Bárdossy, 2003, Jetten, 2002).

Figure 4.4: Contribution of sub-catchments to the discharge into the rice fields.

The contribution of the main channel (C01) to the catchment hydrograph is high. Catchment C09 has a 30 minutes time to peak, which is also half an hour earlier than the rest of the sub-catchments which have no lag time at all since the same time of peak rainfall is recorded to have the peak discharge. This seems to be a result of lumped hourly rainfall thereby making an exact time of maxima for both the input and response variables difficult to determine. However, this may imply that the quick response of the catchment, combined with the velocity of flow, causes immediate and sharp rise of C01 earlier than the rest of the catchments. The time to peak flow, defined as the time from start of rising to peak discharge according to Wang et al (2008) is 5.5 hours with the exception of the noted C09. Note that the simulation in LISEM was started at time (t) = 60 minutes to reduce the computation time. On a similar note, Bronstert and Bardossy (2003) reported that temporal variations

of rainfall play an essential role in the hydrological behaviour of the hillslope or sub-catchment scale especially in infiltration-excess runoff areas as is the case with the study area.

4.6.3. Sub-catchment C01 scenario

It is notable that C01 from the northern mountainous slopes has the largest influence in the hydrology of flash floods in the catchment (Figure 4.4) amongst four other sub-catchments hydrographs of the sub-catchments. C01 covers over 27% of the area of the entire catchment. It also has the steepest slopes, making its flow velocity high of the discharge ideal hence trigger flash floods. It has a predominantly dense forest land use, which imply high interception. However, the effect of vegetation in the rainfall-runoff process identified by van Dijk and Bruijnzeel (2001) is exceeded by rainfall intensity to result in runoff. Under these high intensity rainfall circumstances the steeper slopes, as is characteristic of C01, is an ideal topographic factor promoting the generation of runoff.

4.7. SOBEK model

Sobek 1D2D simulation is based on the saint Venant's equations based on the conservation of mass, energy and momentum as described in the literature review. For a more detailed explanation of these and the construction of the network refer to Alkema (2007) and Sobek Online Help. The outline of the schematisation is presented in Section 4.8.

4.7.1. Sobek scenarios

The use of the data base created for SOBEK simulation included the discharge hydrographs from the 34 sub-catchment scenario into the SOBEK upstream boundaries. Three scenarios were simulated.

Flood modelling in the rice valley fields was then done using SOBEK 1D2D flood model. Three scenarios were attempted, one with natural slope and two with modified slope; terraced and terraced with some breaching dikes in the rice fields. The illustration of the DSM schematisation is as shown on Figure 4.5.

- **Dike-break scenario**

The scenario schematised the DSM as terraced with 0.5m higher dikes than the surface. This attempted to represent the field observations on the dikes in the rice fields that were also observed to have signs of cracks hence hypothesised to break under a severe storm event. The terraces were 1m high and to simulate breaking dikes, the respective dike-pixels were raised by 0.5m above the terrace as illustrated shown on Figure 4.5a.

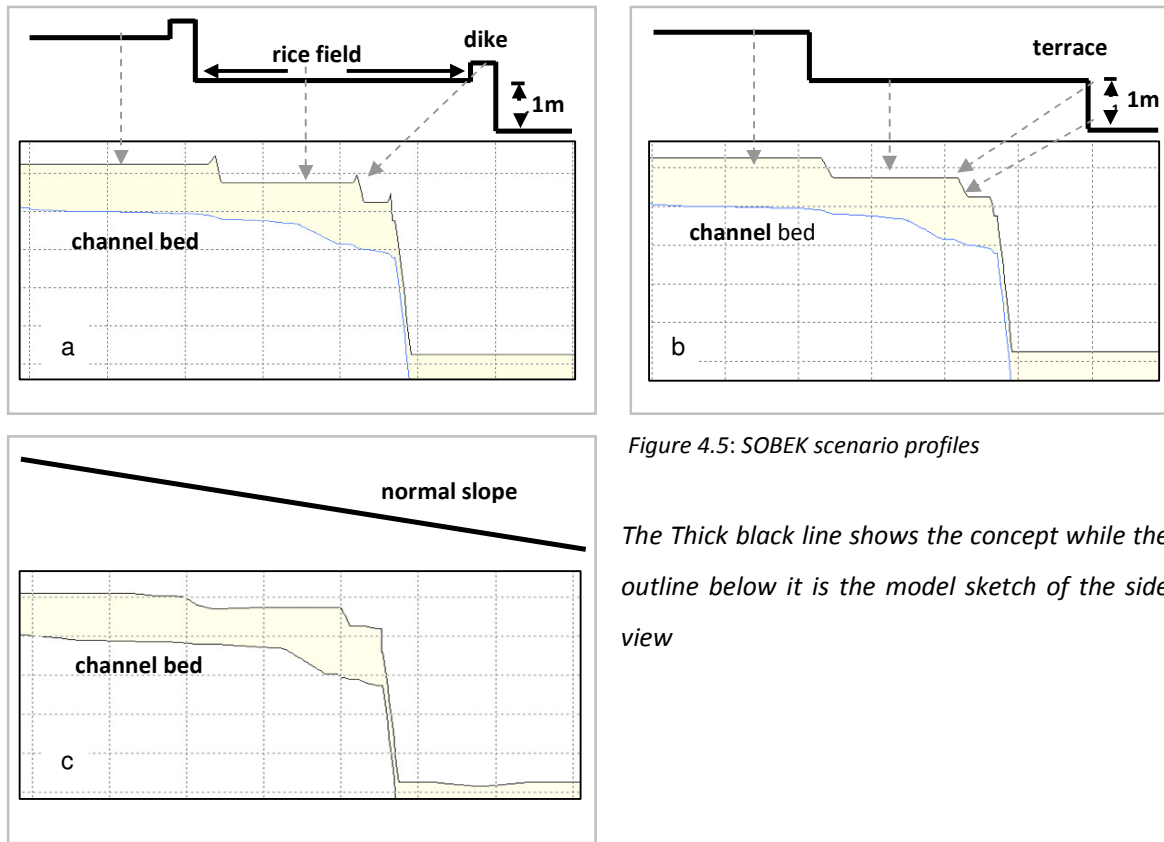


Figure 4.5: SOBEK scenario profiles

The Thick black line shows the concept while the outline below it is the model sketch of the side view

- **Terraced slope scenario**

This scenario was similar to the dike break except that dikes were removed from the schematisation. The terraces are also prominent features in the rice fields as shown on Figure 3.11 which is an important terrain modification evident in the catchment.

- **Normal slope scenario**

This scenario was meant to understand what would happen without the above-noted terrain modifications in the rice fields. This scenario was also important for the further analysis of the performance of LISEM compared to SOBEK using the comparable features of discharge.

- **C01 scenarios**

The main channel only scenarios under the three above terrain scenarios were also simulated after realising the influence of the main segment. The hydrographs of the LISEM runoff scenario for the 34 sub-catchments led to this further simulation set.

4.8. Schematisation

From the eight task blocks that constitute SOBEK model noted earlier, the ‘Schematisation’ is the stage where the network is set using the data as noted earlier (Section 3.2.2). The schematisation is

done using nodes and connectors on the netter interface. A summary of the schematisation in the study is presented on **Table 4.4**.

Table 4.2: Summary of the total nodes used to schematise the model.

Network node	total	change
Flow Connection	33	fixed
1D Flow Boundary	35	fixed
Flow Calculation Point	1 654	fixed
Flow Measurement Station	25	fixed
Flow Cross Section	210	adjusted
2D Grid	(3)	adjusted
2D History	6	fixed
2d Breaking Dam	20	adjusted
2d Corner	6	fixed
Initial Water Level	18	adjusted

In addition to the tabulated network nodes, three 2D Line boundaries at the downstream side of the catchment were added to the network.

For each of the nodes tabulated, the flow connection, flow calculation, flow measurement station, 2D grid, history and 2D

corner were less demanding than the 1D flow boundaries initial water levels and flow cross sections that were adjusted for each individual scenario. Therefore as such the cross sections, initial water level and 1D boundary conditions, breaking dam nodes are presented below.

4.8.1. Cross sections

Using the cross section tab in the NETTER, 1D cross section node (Figure 4.6 a) was digitised and the shape and geometry (Figure 4.6b) were defined. The location coordinates were default values while the bed and surface levels were user defined (Figure 4.6c) was, and friction values were added into the scheme of the model.

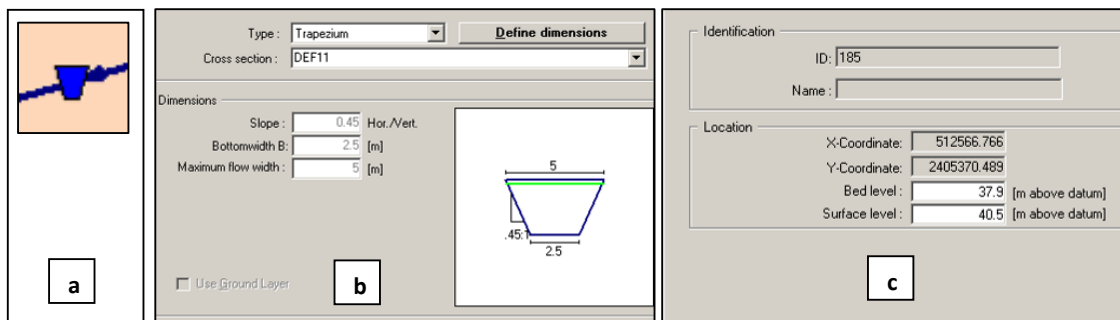


Figure 4.6: Cross section node (a), shape and geometry (b) and the location details (c)

The location of the measured cross sections is in Section 3.4.3 (Figure 3.6). Coordinates and ID of the cross section were accepted as default values while the surface and bed levels were defined as guided by the DSM. The trapezium shape of cross section was selected following the field observations on the general shape of the channels. Slope, bottom and surface widths were defined as shown on the example on Figure 4.6. The channels friction value was fixed manning's $n = 0.03$).

4.8.2. Boundaries

For each of the 34 upstream 1D boundaries, the discharge table was imported from the LISEM output to introduce the hydrograph that was an important input into SOBEK. The table covered a 12 hour time from the start of the storm event

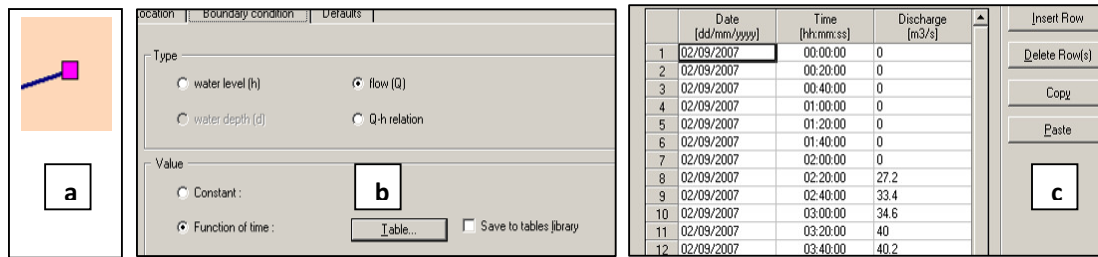


Figure 4.7: 1D boundary node (a), boundary condition definition (b) and discharge table (c)

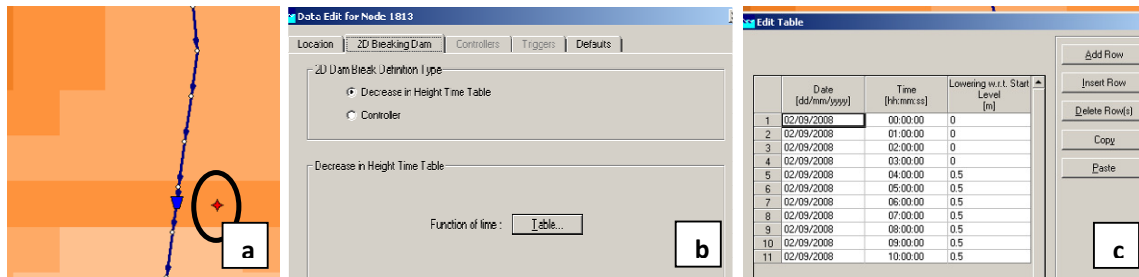


Figure 4.8: Dike-break node (a), node definition (b) and dike-break timetable (c).

The dike-breach was modelled using a time table to allow the breach one hour after the 56.4mm rainfall intensity per hour had begun. This simulation was necessary following field observations and interviews with the local people that revealed that some dikes break during large storm.

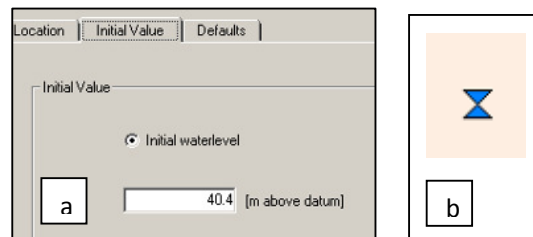
4.8.3. Initial water level

The initial water level in the rice field and the definition of the node in the schematisation are as shown on Figure 4.9. The rice fields were observed to be under water during the field work hence the need to include the initial water level in the schematisation of the flood model. The water level had to be adjustment in view of the changing surface levels as a result of terraces.

Figure 4.9: Initial water level input tab (a) and its node (b) for each simulation.

4.8.4. Dike breaks

The dike-break simulation can also involve overflowing effect before the breach as a result of the volume of water flowing down, which is also an important interview outcome. Due to some the loose gravel and sands on some of the dikes, the break is likely to occur during an intense storm as a result of some openings as observed during field work.



The effect of the dike breaks were simulated using 0.5meter dike crests that were lowered to the surface level using a dike-break time-table as outlined in Chapter 4. Figure 4.21 shows a dike-break situation, before and after the break. Before the break (Figure 4.21a), the dikes have a storage effect. Upon filling up, they overtop and break releasing a huge volume of water that cascades downslope under gravity as a flood wave. Dike-break time table was created based on the enormous increase of discharge on the LISEM hydrograph triggered by the sudden increase in the rainfall intensity from 2.5 to 56.4mm/h. The breaking and overflowing dike is shown on Figure 4.21b simulation based on main stream discharge releasing a flood wave into the middle level paddy. The velocity is also high as the length of the arrows show on the pixels.

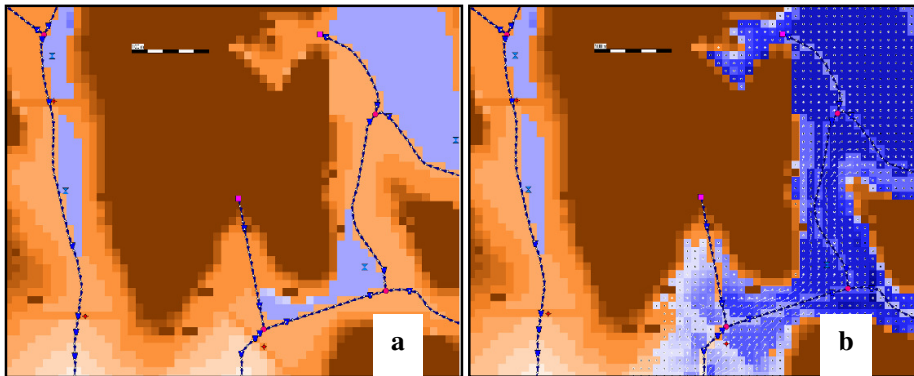


Figure 4.10: Three dikes with dike-break nodes (red stars) before (a) and after (b) the dike-break (b).

The result of the schematisation is shown on Figure 4.10 with full network.

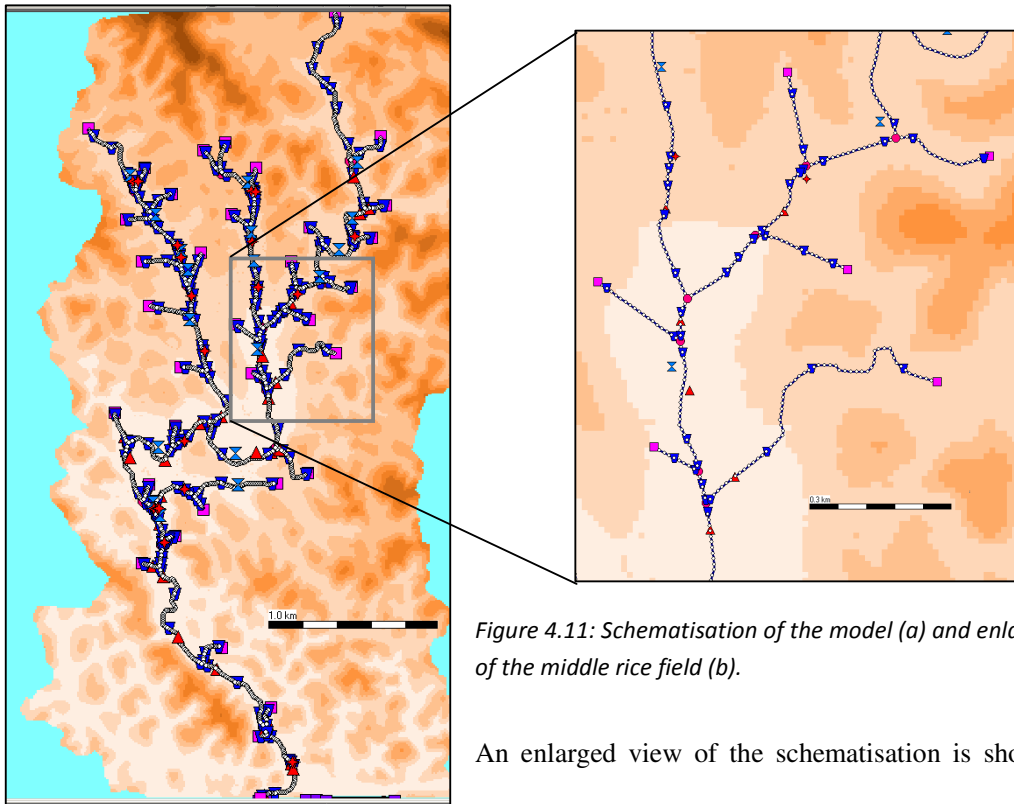


Figure 4.11: Schematisation of the model (a) and enlarged view of the middle rice field (b).

An enlarged view of the schematisation is shown on the

right hand side

As defined in the ‘Settings’ task block where one minute simulation and 10 minutes output time steps were set respectively. The assumptions in the 1D initial (Rural) module settings were maximum embankment of channel, unsteady calculation and completely dry river system. In the Overland flow (2D) module the same embankment assumptions and output definitions were made.

4.9. Sobek model results

A summary of the modelling results by scenario is presented on Table 4.5.

Table 4.3: Summary of flash flood simulation results

PARAMETER	SCENARIO		
	Dike break	Terraced slope	Normal slope
Flood extent (km ²)	1,2	1.1	0.9
Mean depth (m)	1.1	1.4	1.0
Time to peak discharge (h)	3	2.5	2.5
Maximum depth (m)	4.15	4.19	5.86
Maximum velocity (m/s)	4.23	2.75	2.73
Maximum impulse (m ² /s)	6.95	4.16	5.11

A summary of characteristics of each SOBEK scenario is presented on Table 4.7. On the same note, Figure. 4.11 depicts flood extent and depth by scenario. Maximum flood extent is predicted to be highest and lowest in the dike-break and terraced slope scenarios respectively (Figure. 4.11 and 4.12a).

The dike-break scenario predicted the largest flood extent and recorded the fastest flow while the deepest areas exceeding 5.5m where predicted in the normal scenario. The terraced scenario is consistently intermediate except for maximum impulse where it is lowest. The implications derived from such results suggest that dike-break scenario poses the greatest threat due to high impulse. More detail of the spatial effects of these parameters is presented in the following sections.

4.10. Topographic scenarios

4.10.1. Flood Depth and Extent

Flood depth is important to define in flood studies is in defining extent and cost of damage. The respective depths at the exit of the catchment were noted for the three respective scenarios. The areal extent of the flood is consistent with a longer ‘tail’ downstream on the dike break scenario that emerges on the terraced and dike-break scenarios. In all the scenarios, the middle paddy shows the largest spatial effect of the flood.

According to Alkema (2007), a combination of flow depth with flow velocity is important especially to determine the amount of potential damage. The distribution of the flow depth in the three scenarios is as shown on Figure 4.11 with areas of deep flood shown in deep blue while shallow water is green respectively on Figure 4.11. The dike-break scenario shows moderate depths in the same areas which

are deeper in the terraced with even ‘deeper spots’ are more evident in the normal scenario. Terracing the slope has an effect of filling up the depressions with a significant depth as was also observed during field campaign. This confirms why middle paddy is shallower and the lower deep part of the paddy is reduced in size while the upper agrees with the normal slope scenario as shown on Figure 4.11. Water depth has implications in disaster related assessments as it relates the amount of danger and potential damage, with deeper flood affecting more elements at risk (houses and properties) than shallow (Alkema, 2007). It is important to note as Leenders et al (2009) forwarded that depth has perhaps the strongest influence on flood damage and concluded that it was therefore very relevant to characterise flash flood damage areas or those near dike breaches.

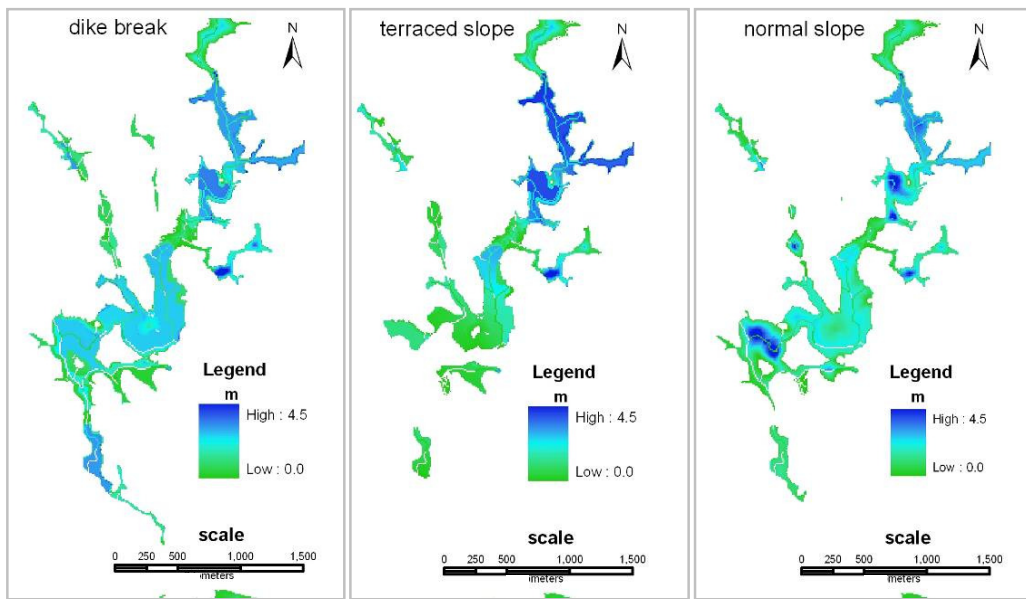


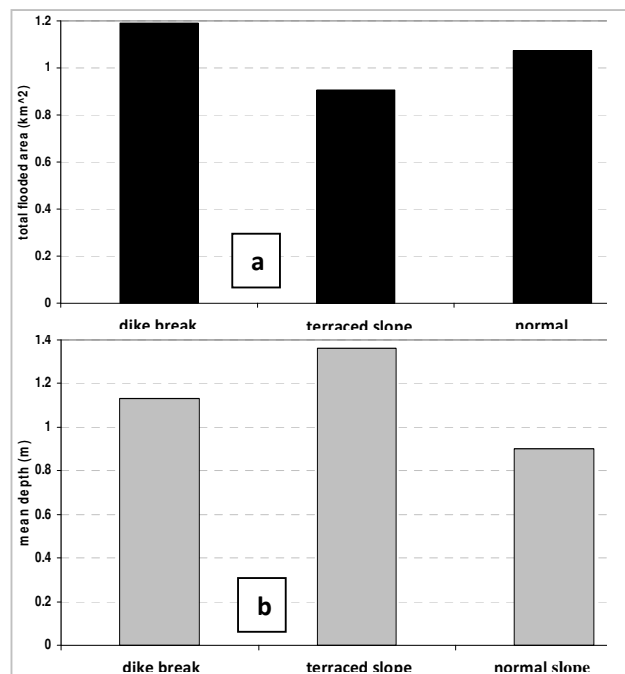
Figure 4.12: Maximum depths (m) simulated with three SOBEK surface terrains.

In the three scenarios the deepest flood is predicted to occur as a result of the terracing slope (Figure. 4.12b). The average flood depth is simulated to be highest in a terraced scenario and lowest the normal slope scenario as shown on Figure. 4.12b. This is influenced by the lowest area flooded.

Figure 4.13: Flood extent (a) and flood depth.

4.10.2. Maximum Flow Velocity

The maximum velocities in the study area under a flash flood triggered by a high



intensity storm event of same magnitude is predicted to be as shown on Figure 4.13. This parameter was higher in the dike-break scenario as shown on Figure 4.13. However, the dike break scenario as shown on Figure 4.13 has a larger influence of increasing velocity at these hot spots. More velocity ‘hotspots’ are also noticeable further downstream than the other two scenarios predict. As presented on the dike-break Figure 4.13, the effect of the breakage of the dike is evident hence such higher velocity associated with the breaching dikes is not surprising. It is noticeable that these velocity hotspot areas are influenced by the bottleneck at or immediately upstream. However, the curved rice fields downstream of these hot spots depict an ‘absorbing effect’ and reduce the velocity as shown on the Figure 4.13.

As shown on Figure 4.13, the ‘hot spots’ of maximum velocity (red) are determined by the slope of the terrain in conjunction with the bottlenecks. As the flood waters reach the wider downslope fields, the velocity immediately decreases. Maximum flow velocity hot spots were consistent in the three common areas of high slope angle except for additional areas down slope as in the dike break scenario. However, the dike-break scenario shows larger areas of higher velocity as compared to the terraced and normal slope scenarios. Flow velocity has been elaborated by Alkema (2007) as the force of the flood water to sweep off people, especially the more vulnerable children and elderly, off their feet is determined by the velocity parameter. Leenders et al (2009) also concurred that high velocities lead to increased damage.

4.10.3. Maximum Impulse

The product of flow velocity and depth gives impulse (Alkema, 2007) which helps in characterizing potential danger a flood event poses in view of high velocity and deeper flows being more dangerous. As shown on Figures 4.13 and 4.14 maximum velocity and impulse occur at the steeper part of the terrain as well as on the bottlenecks. The side profiles on the SOBEK results reveal that these areas of higher velocity are areas where the terrain of the valley attains highest slope angles. The influence of velocity on impulse is more evident than that of depth parameter. Elements at risk in the high impulse areas are more vulnerable than out. However, the risk in this case is potential loss of rice crop in the catchment if the occurrence of the flash flood is prior or at harvesting time.

The respective hydrographs of the three scenarios are presented on Figure 4.15 showing the dike-break scenario as a worst case that doubled the amplified of the discharge wave. The other two scenarios have a similar response with double peaks although the normal slope has a more subdued second peak as compared to the terraced slope. This behaviour of the double peaks depict a flash flood that occurs in two waves separated by three hours of peak flow. While all the three scenarios show that until the 4th hour, (5th hour of the storm), the spontaneous increase of discharge in the dike-break scenario is attributed to the breaching of the dikes as their break was initiated on the fifth hour

according to the dike-break time table. The dike break shows an earlier lag of 1 hour while the second peaks of the terraced and normal scenarios are 2.5 and 3 hours respectively

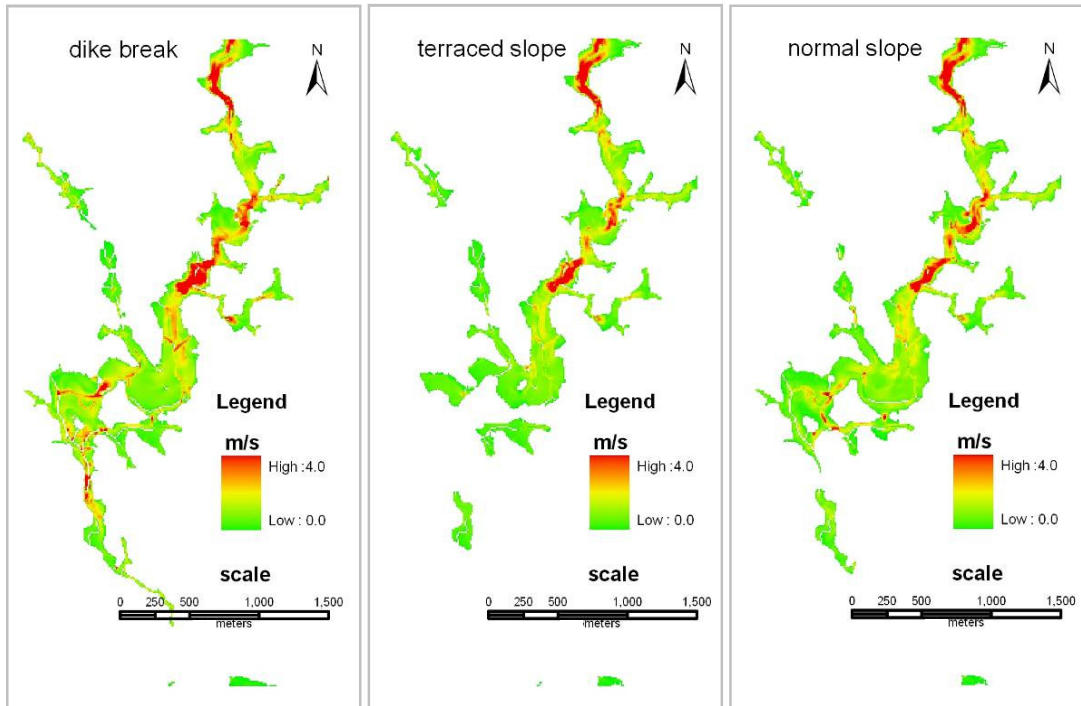


Figure 4.14: shows the distribution of the maximum velocity by flood scenarios.

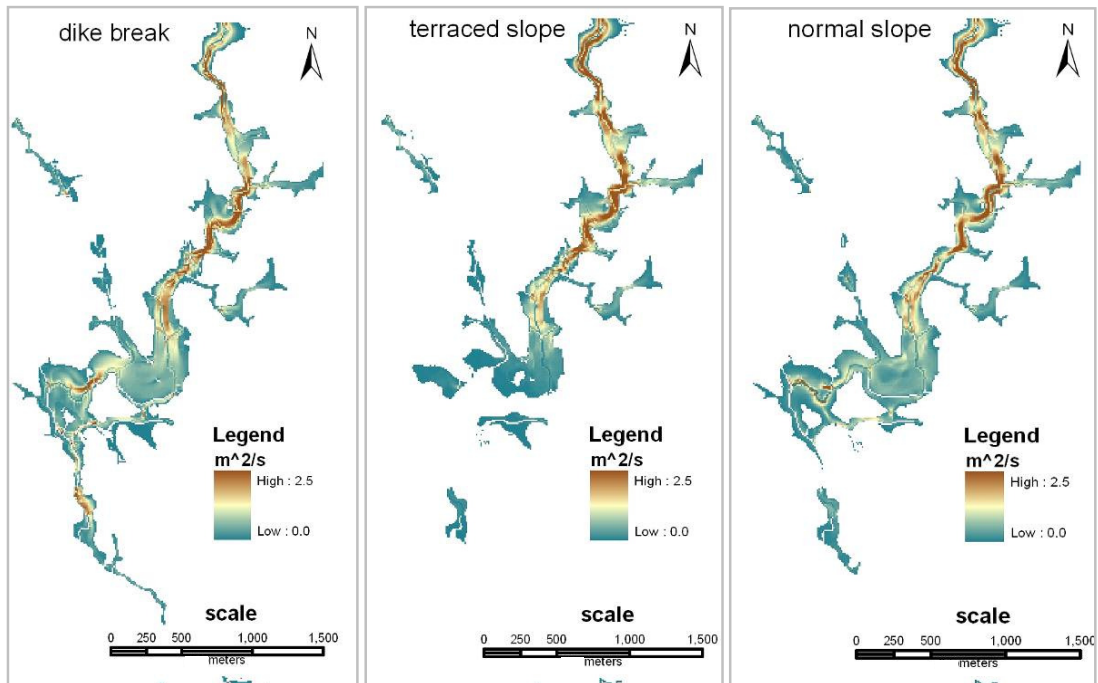


Figure 4.15: Impulse with respect to the three scenarios.

4.11. SOBEK flash flood scenario hydrographs

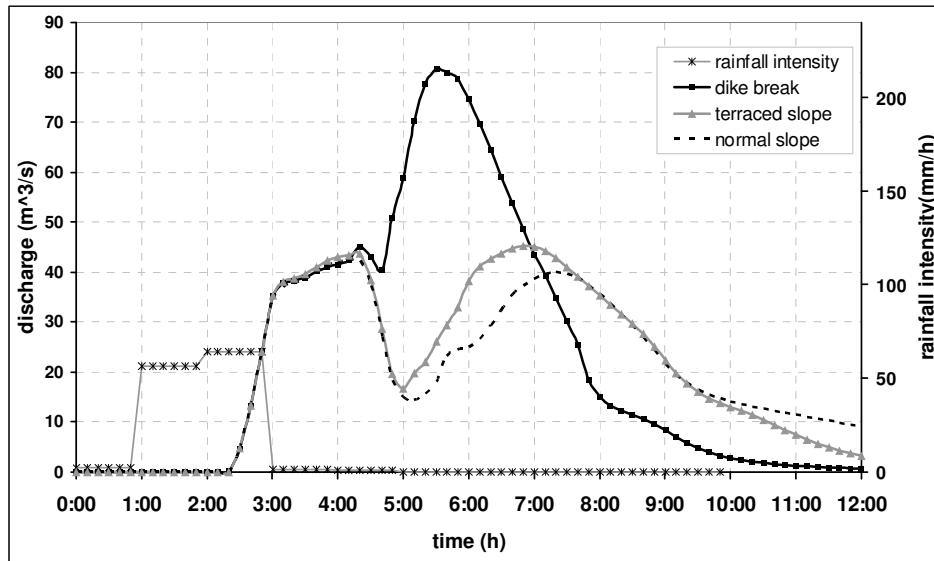


Figure 4.16: Hydrographs for the three SOBEK flood scenarios

The subdued peaks of the flash flood simulation shows that there is a lot of buffering in the catchment as the terraces detain the water in addition to the huge volume of storage. The storage effect is shown on Figure 4.17. The storage function of the several mapped ponds and the reservoir, ponds calculated to hold approximately $675\,000\text{m}^3$ of water in addition to the ridges and depressions in the rice fields as shown on the food depth maps of the three scenarios. The small ridges, canopy storage and unbroken dikes as well ponds reduce the water available for discharge generation. The area seems to have a 'local' flood that dies down or is detained at the centre of the catchment due to the winding shape of the valley as shown on by the winding river on Figure 3.18. The geometry of the rice fields as well as the terrain to cause a 'meander-like' neck that thrusts the water and then detain it in the area. The configuration of the terrain causes a screwing effect and traps the flow in the loop and in that case acts positively to reduce the downstream flood potential hazard. Worth noting is the buffering effect as evident on the middle paddies where the flood wave the wave is thrust upslope and diverted due to highland obstacles and the flow screws hence reducing the impulse and retaining the water for a while. While this reduces the flow velocity down stream, the areas in these zones are however inundated deeper and larger spatial extents. In a related study downslope by Alahacoon (2010) using the above two hydrographs; a smaller flood was simulated in Yen Bai city. The dike break produced larger spatial extent as compared to the normal slope scenario.

4.12. Catchment Water Balance

The inflow in the three scenarios was the same. The outflow and storage were different (Figure 4.17) scenario.

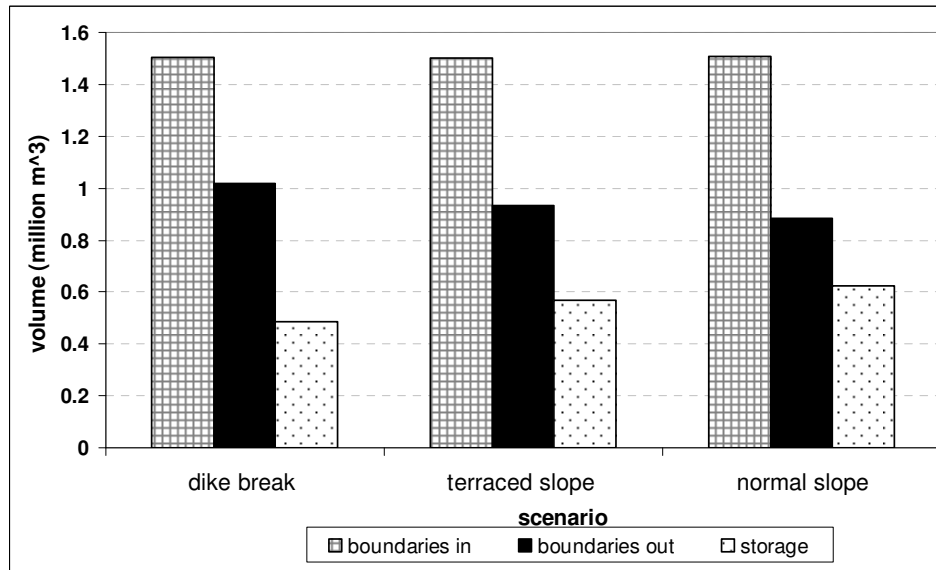


Figure 4.17: showing the water balance in the catchment with respect to the three scenarios.

The three scenarios showing the volume of water into and out of the catchment are presented as line graph on Figure 4.17. The volume out of the catchment is low during the scenario with terraces only while the dike and normal slope scenarios reach the same level at different times. The terraced and dike scenarios tend to level out at maximum earlier than the scenario with the current terrain. The difference between the dash-dot line (inflow) and the solid lines (outflow) shows an increase in the stored in the catchment from the 2.5 to 5 hours after which the upstream boundaries remain constant. The total volume between the terraced and normal slope scenarios narrows down while that of the dike-break is distinct showing less storage than the other two. The dike-break scenario has the highest volume reaching the outlet confirming its worst-case scenario as exposed above than the other two with half the peak discharge as revealed on Figure 4.18.

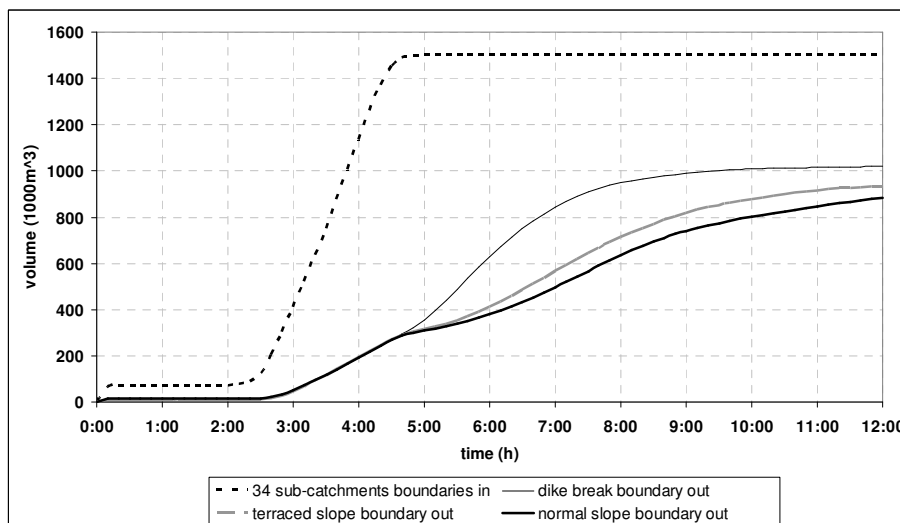


Figure 4.18: Cumulative volume at the downstream boundary for the three SOBKE scenarios.

As shown on Figure 4.18, there is more volume out of the catchment under the dike-break scenario implying in less storage. The reverse is true for the normal slope scenario. However, the response of the catchment to the flood wave is not very distinct in terms of volume. This is a result of the terrain which resembles the level fields in all the cases as schematised on Figure. 4.5. Although the terrain was simulated differently, it shows that all the three scenarios show almost similar surface expression except for the outstanding dikes, which drain the catchment of more water when they break. As observed during the field campaign, the catchment has buffering effect due to dikes as well as three curves at several points on the valley (Figure 3.6). Eight bottlenecks were noted in-between the main channel upper and lower boundaries as represented on Figure 4.11. These bottlenecks act as 'hydrological valves' regulating the flow at these areas. The areas of these curves also reveal a breaking effect as the higher velocities reduce upon reaching these segments and also retain water for longer. The bottlenecks at below flow velocity breaking curves increases the temporary storage time at the bowl-like features in the catchment. The storage effect of the catchment is large. A calculation of the total volume stored by the mapped water bodies with dam ($189\,600\text{m}^2$) and ponds ($295\,000\text{m}^2$), estimated the storage by $675\,000\text{m}^3$ to yield a volume balance of around $800\,000\text{m}^3$ almost tallying with the model results.

4.13. Applicability of LISEM as a Flash Flood Prediction Tool

An assessment of the flash flood hydrograph as simulated using two models is presented. LISEM shows a lag of half an hour while SOBEK predicts a one hour lag of the same magnitude for the first peak and the second peak discharge occurring four hours later. The discharge of LISEM is three and half times amplified as compared to the SOBEK natural terrain scenario. This implies that LISEM prediction shows a kinematic wave that sharply rises in one and half hours to occur in only two hours while SOBEK has a lower and double peak flood wave. The implications of the LISEM model therefore shows that the warning lead time has to be short and signifies a more rapid wave unlike the gradual one in SOBEK scenario as shown on Figure 4.18

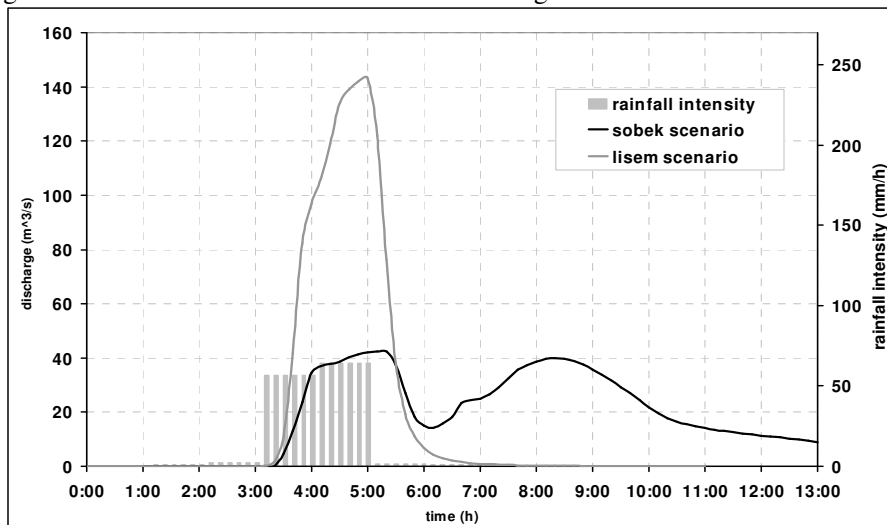


Figure 4.19:
Hydrographs for
SOBEK, LISEM whole
catchment and CO1
scenarios

The total volume leaving the catchment is 10% more from the SOBEK scenario than the LISEM scenario. A possible explanation for this loss of water in LISEM is infiltration on the rice fields as illustrated on Figure 4.19. SOBEK does not lose water through infiltration hence more volume outflow in the SOBEK scenario. It is evident, however that the performance of the two models show close prediction in the volume of water leaving the catchment. The difference is presented on the LISEM SOBEK hydrograph on Figure 4.17, is that the LISEM kinematic wave is shorter predicting a flood of two hours unlike that from SOBEK where the wave takes six hours to rise and recede at consecutively.

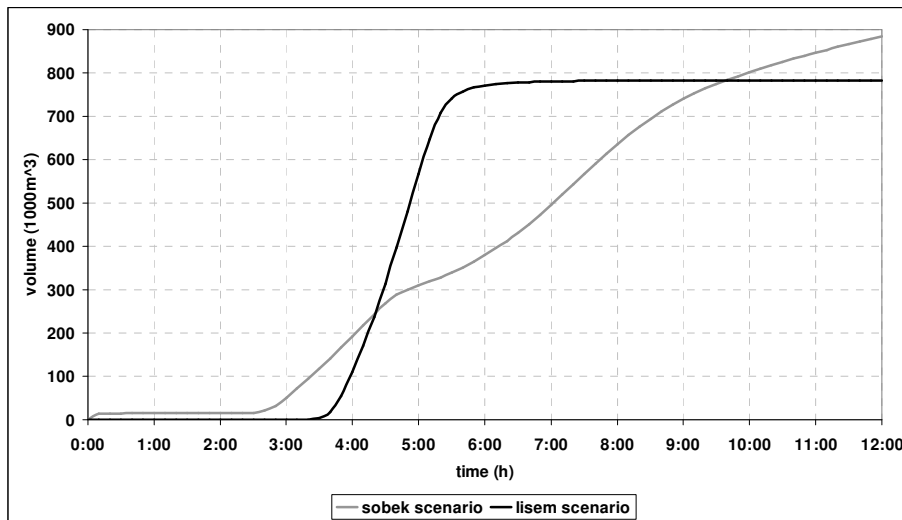


Figure 4.20: Comparison of the predicted cumulative volume for the two models.

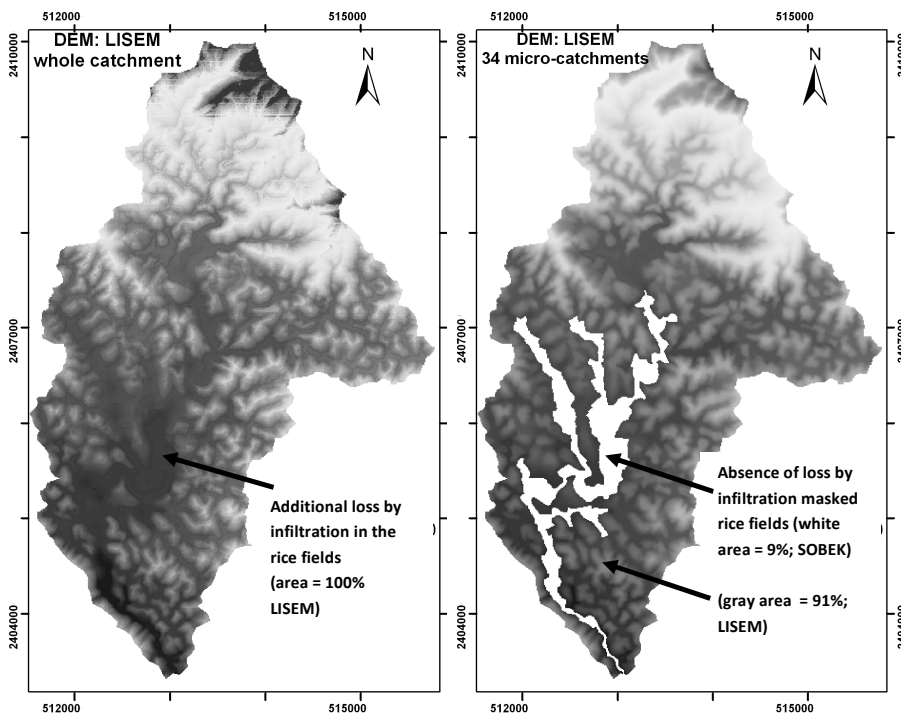


Figure 4.21: Infiltration influence on predicted volume

The results of the LISEM and SOBEK normal slope scenarios were assessed at 10 minutes interval and the curves of the cumulative volume of the simulations is shown on Figure 4.20.

Using one DEM, the SOBEK and LISEM scenarios results of cumulative volume are presented on Figure 4.20. The LISEM scenario shows a sharp increase in the volume of water reaching the catchment outlet while SOBEK has a lower rate. The total volume output of LISEM compares well to that in SOBEK except that the former reaches the maximum after only two hours. The use of LISEM to predict flash floods is possible but the accuracy requires use of real discharge data to calibrate and validate the model. Accuracy of the model required application of discharge data. It shows that LISEM is capable of being used as a flash flood forecasting tool in this catchment. However, while there was lack of discharge data, model calibration used interview discussions.

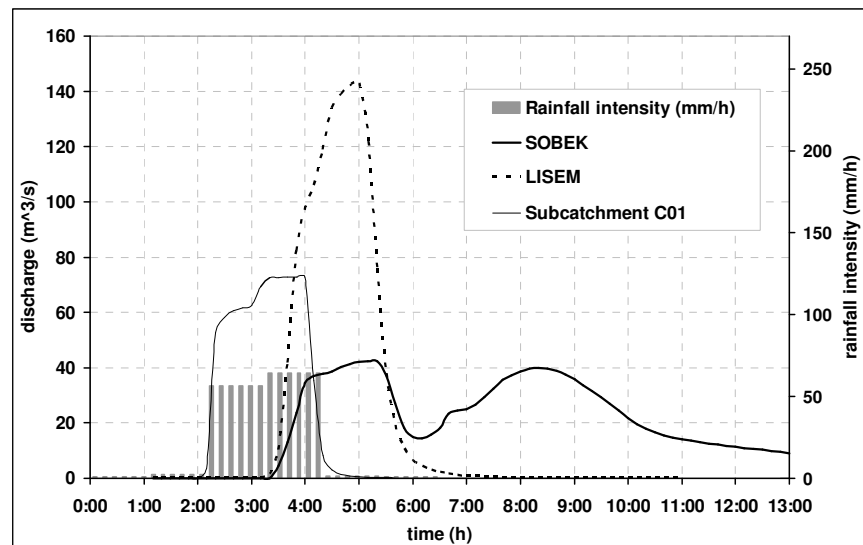
This implies that using a LISEM scenario, for a flood triggered by such a storm would mean that the rise of the water level in the area is recorded two and half hours after the onset of the storm, with the sudden rise triggered by the high intensity. A more swift warning and evacuation time is required if the flood wave behaves in the way as predicted using the LISEM scenario. While the SOBEK scenario simulates a more gradual rise taking five more hours to reach the same volume.

4.14. Influence of the C01

LISEM scenario with 34 sub-catchments (Figure 4.22) revealed the influence of C01 in the catchment. As a result, three terrain scenarios using C01 only discharge were simulated to detect the influence of the sub-catchment to the entire catchment. The hydrographs of the three scenarios shows a large contribution of the sub-catchment with a peak nearly twice the first one of the SOBEK scenario. To understand further the double peak discharge on the hydrographs depicting two flood waves three C01 scenarios were run and the respective results are as shown on Figure. 4.23.

Figure 4.22: C01 effect on the volume outflow for the three scenarios

There is a consistency in the SOBEK results showing a gradual increase of volume for the terraced and normal scenarios while the



dike-break scenario has a faster rate of increase to level out one and three hours earlier than the terraced and the normal slope scenarios respectively. This is not surprising as the side views of the terrain (Figure 4.3) showed that the terraced and normal slope scenarios have almost similar slope characteristics. However the dike-break scenario shows more discharge at the 12th hour after the start of the simulation while the terrace scenario is lower and assuming a parallel behaviour to that of the dike-break scenario. The difference between the boundary inflow and the outflows reveal the amount of water stored in the system, which is greatest with the terraced scenario. An increase in the fifth hour reveals that the main catchment is influential.

On all cases, it is notable that the response of the main outlet shows a delay of about two hours. A normal slope delays the flood wave by 30 minutes and reduces the discharge peak by 50% under the simulations done. It should also be noted that the discharge recedes back to baseflow level earlier in the dike scenario (red) than the normal slope scenario (blue). However, the outlet rises in the water depth to remain at a constant 5m depth during both simulations with a rapid rise from baseflow level to 5m in the first quarter of an hour of the start of the simulation period. The two scenarios showing the dike and natural slope situations show a consistent cumulative outlet volume of 250 000 m³ but the rate of increase is faster and levels out in the dike-break scenario than the normal slope which increases gradually but at the same end of simulation period.

4.15. Summary

Upslope areas are predominantly plantations with tree crops including tea and cassava. These land covers have a higher percentage cover than the rice fields in the valleys. The saturated hydraulic conductivity of the area did not seem to be influenced by either land use or lithology as was assumed. The main channel is the largest discharge contributor in the catchment as demonstrated by the hydrographs from both the 34 scenario and the main channel scenario in LISEM and SOBEK respectively. The terracing and dikes on the rice fields makes the natural slope complex and has implications of increasing the flood extent. Dike-breaks amplify the flood peak and shorten the high flow duration. The catchment responds promptly to severe storm. The bottlenecks and the valley flows also delay the flow thereby inundating the area for longer than without them.

5. Discussion, conclusions and recommendations

5.1. Discussion

The results presented starting on Section 4.9 are discussed below.

The catchment has shown a spontaneous response to a high intensity storm event regardless of the high K_{sat} and moderate porosity. Both LISEM and SOBEK have revealed a fast response to reach the catchment outlet within 4 hours with a lag of 3 to 4 hours respectively. The catchment yields a significant amount of runoff of almost 50%.

The paddy fields are generally low lying and of very low slope angle, therefore there is inundation of the rice fields to higher depths and wider areas. Field work observations noted that the valleys prone to flooding are basically rice fields and vegetable gardens. The elements at risk therefore is the paddy crops largely rice especially as the storm analysis has shown the largest rainfall potentially occurring in august as shown on Figure 1.2. In the rice fields, ponds and dikes noted during the field campaign and simulated have an important storage effect. However, a high intensity rain event with a large depth may cause the dikes to break and cause a shorter but high flow that floods a larger area than without the breaches.

The dike-break has shown an amplification effect on the peak discharge of the flows (Figure 6.5). It is however, notable that the buffering effect of the paddies is reflected on the first subdued peak when downstream discharge recorded is over-spilling of the dikes and ridges in the catchment. The second peak is a delayed flow from a long segment which is more likely C01 due to the distance to the outlet. When the second wave arrives, the fields are already full and consequently the second wave proceeds towards the exit of the catchment, hence the more pronounced peaks on the SOBEK outlet node. The double peak behaviour of the catchment is seems to suggest influence of two regions of which C01 is one such candidate as the simulation has revealed. Discharge data for the segment would be ideal to check the hypothesis. The findings on the influence of dike-break in the study revealed that failures of dikes result in faster flow velocities and consequently impulse as revealed on the flood results. This result is consistent with those by Alkema (2007) on a more detailed study on the ‘Ziltendorfer Niederung’ flood who concluded that without dike breaches, overtopping and flooding was not going to occur. In this study, the higher velocity was a result of the higher slope angles on the parts of the rice fields as well as the bottlenecks as presented above. Therefore the effect of dike-breaches in the flooding of the area is important to note.

The two subdued peaks in the terraced and normal scenarios implicitly represent a less severe flood event than resulting from either the LISEM prediction which has a third of the duration and treble discharge amplitude. LISEM predicted shorter duration revealing a self-propelling effect of the kinematic wave typical of a 1D model that cannot dissipate the flow in 2D. The dissipation of energy and momentum in SOBEK leads to longer duration as the reduced velocity causes more travel time that thrusts forward due to the column of water accumulating on the pixel and leaving in only one direction. LISEM therefore registered shorter duration as revealed. High velocities were revealed (Chapter 2) to be important in the potential damage (Alkema, 2007, Leenders et al 2009). Furthermore, the curve winding shape of the rice fields also break the velocity and enhance the storage time. Both models predict a higher discharge with the LISEM twice that of the dike break scenario of SOBEK. LISEM predicts a flash flood that is thrice in discharge amplitude and one third duration. It should be noted that the total volume recorded from the two models are very close except for the highlighted infiltration loss in the LISEM whole catchment scenario. Although both models predicted a short response of the catchment flow, it should be noted that the two are different. They reinforce the need for a short response time hence reinforces the necessity for an effective communication of the flood hazard as mitigation.

While the above points have been noted, it should also be recognised that the simulation was not adequately calibrated due to lack of real discharge data on the catchment. The calibration that was attempted was not successful since the time period of the storm isolated was noted to have other influences including pumping out of the water from the upstream reservoir as later learnt. While there was a significant historic record of rainfall at daily resolution (1960-2009), the discharge data is the main modelling constraint in the catchment. Therefore the reference to the runoff coefficient may not be the most ideal although it was found to be appropriate as Kinoshita (1983) also found out that it could vary from catchment to another. The results reveal that with the necessary discharge data, LISEM is potentially applicable as a predicting tool in the catchment, although the duration was noted to be different from that of SOBEK. However, adequate calibration has to be practiced due to the 1D assumption noted above.

Model predictions based on the analysis of the modelling processes show that with a short duration storm lasting a few hours with a concentrated amount within an even shorter time period hours has a potential to trigger a runoff and is potentially capable of triggering a flash flood. However the exact quantitative values could not be ascertained due to lack of discharge data for a proper calibration and validation of the model results. The main stream is an important 'indicator' that could be quantified with the necessary data. The location of the upstream diver in the catchment is potentially a strategically positioned and therefore could lead to the quantification of such a relationship. However the modifications and developments in the downstream paddies should as well be noted consistently

for disaster management implications. Despite the limitation of discharge data necessary for an intensive analysis, the results show that high intensity rainstorms combined with breaking dikes may cause a worse flood than without the dike breaks. The field observations noted that materials used to build the terraces varies from unconsolidated gravels to compacted clays. There is no prescription on the type of material to build the dikes as field campaign has shown.

LISEM simulations revealed that the catchment has a high runoff yield if a severe storm is experienced despite the high infiltration and interception losses on the slope areas. This kinematic wave ends up in the valley flows where a flash flood is propagated due to the complex features in the valleys simulated using SOBEK. In this regard, effective communication and monitoring of the progress of storm events for the real time forecasting is important as noted earlier (Imamura and To, 1997; Sorooshian, 1997; Kelsch, 2001; Rientjes, 2004 and Norbiato et al, 2008). While LISEM shows a faster and shorter wave as depicted by a narrower and more pronounced peak histogram, SOBEK tended to have two peaks more evident in the terrace and normal slope scenarios with a longer duration of the flow regime for the event. The predicted volume of discharge is consistent between the two models although the duration of the high flow differ greatly. The coupling of the LISEM version 2.62 Beta (Jetten, 2010, personal communication) compatible with the SOBEK input requirements have proven great success as a flash floods test-case of Cuong Thinh Catchment of Yen Bai in Vietnam.

5.2. Conclusions

In view of the questions asked (Chapter 1) in order to understand the trigger mechanisms of flash floods, data was collected (Chapter 3) and analysed before applying in the two models (Chapter 4) to come out with the following conclusions;

Question 1: *What are the land use and soil physical properties in the catchment?*

Answer 1: Forest and plantations are the major land uses (80%) on hill slopes and rugged terrain. Patches of tea plots are also noted. Rice (9%) is the main crop in the valley flows. The catchment has very moderately high saturated hydraulic conductivity and moderate porosity.

Question 2: *What is the contribution of the upslope and the rice paddies land uses in the runoff generation and propagation of the flash floods?*

Answer 2: The up-slopes generate a wave that propels down-slope into the valleys. The shape and slope of the rice fields and dikes constructed buffer the flood, but if the dikes break, the flood rises quickly amplifying the peak discharge and while inundating more area than without the breaching.

Question 3: *How applicable is the LISEM in combination with Sobek to model flash floods in this catchment?*

Answer 3: LLSEM was appropriate to model the runoff on the slope but could not handle the flood propagation in the complex terrain of the rice fields which SOBEK was capable of making coupling of the two appropriate in this test case.

5.3. Recommendations

In view of the above conclusions, this study recommends the following;

- Calculating the flash flood index for the catchment is crucial for flash flood mitigation and management.
- Linkage of remote sensing products to reconstruct past events is also important to understand the potential of quantifying the flood characteristics in the catchment using remote sensing methods and products.

5.4. Limitations of the study

- Lack of the discharge data to calibrate and validate the models.
- There was communication constraints.

References

- ABEDINI, M. J., DICKINSON, W. T. & RUDRA, R. P. (2006) On depressional storages: The effect of DEM spatial resolution. *Journal of Hydrology* 318 138-150.
- ABULOHOM, M. S., SHAH, S. M. S. & GHUMMAN, A. R. (2001) Development of a Rainfall-Runoff Model, its Calibration and Validation. *Water Resources Management*, 15, 149-163.
- ALAHACCOON, N. (2010) Flood propagation analysis in an urban environment; a case study in Yen Bai, Vietnam. Enschede, University of Twente.
- ALKEMA, D. (2004) RS and GIS Applications in Flood Forecasting *National workshop on Flood Disaster Management, space Inputs* NRSA, Hyderabad, India, ITC.
- ALKEMA, D. (2007) Simulating floods. On the application of a 2D-hydraulic model for flood hazard and risk assessment. Enschede, International Institute for Geo-Information Science and Earth observation (ITC) University of Utrecht.
- BEVEN, K. (1997) Process, Heterogeneity and Scale in Modelling Soil Moisture Fluxes. IN SOROOSHIAN, S., GUPTA, H. V. & RODDA, J. C. (Eds.) *Land Surface Processes in Hydrology; Trials and Tribulations of Modeling and Measuring*. Berlin, Springer.
- BEVEN, K. J. & BINLEY, A. (1992) The future of distributed models: model calibration and uncertainty prediction. *Hydrological Processes*, 6, 279-298.
- BRONSTERT, A. & BÁRDOSSY, A. (2003) Uncertainty of runoff modelling at the hillslope scale due to temporal variations of rainfall intensity. *Physics and Chemistry of the Earth, Parts A/B/C*, 28, 283-288.
- CHIEW, F. H. S., STEWARDSON, M. J. & MCMAHON, T. A. (1993) Comparison of six rainfall-runoff modelling approaches. *Journal of Hydrology*, 147, 1-36.
- DHAR, O. N. & NANDARGI, S. (2003) Hydrometeorological Aspects of Floods in India. IN MIRZA, M. M. Q., DIXIT, A. & NISHAT, A. (Eds.) *Flood problem and management in South Asia*. Dordrecht, Kluwer Academic Publishers.
- DROBOT, S. & PARKER, D. J. (2007) Advances and challenges in flash flood warnings. *Environmental Hazards*, 7, 173-178.
- DUONG, L. V. & NGUYEN, K. N. (2008) World Vision reaches flood-affected areas in Vietnam 13 Aug 2008
- EIJKELKAMP (2003) Operating Instructions 09.02 Laboratory Permeameters.
- EWEN, J., O'DONNELL, G., BURTON, A. & O'CONNELL, E. (2006) Errors and uncertainty in physically-based rainfall-runoff modelling of catchment change effects. *Journal of Hydrology*, 330, 641-650.
- GIANNONI, F., ROTH, G. & RUDARI, R. (2000) A semi-distributed rainfall-runoff model based on a geomorphologic approach. *Physics and Chemistry of the Earth, Part B: Hydrology, Oceans and Atmosphere*, 25, 665-671.
- HESSEL, R., JETTEN, V., LIU, B., ZHANG, Y. & STOLTE, J. (2003) Calibration of the LISEM model for a small Loess Plateau catchment. *CATENA*, 54, 235-254.
- IMAMURA, F. & TO, D. V. (1997) Flood and Typhoon Disasters in Viet Nam in the Half Century Since 1950. *Natural Hazards*, 15, 71-87.
- JETTEN, V. G. (2002) *LISEM user manual, version 2.x*. Draft version January 2002. Utrecht Centre for Environment and Landscape Dynamics. IN 48 (Ed.). Utrecht University.
- KELSCH, M. (Ed.) (2001) *Hydrometeorological characteristics of flash floods. Coping with flash floods, Environmental Security*
- KINOSITA, T. (1983) Runoff and flood characteristics in some humid tropical regions in Hydrology of Humid Tropical Regions with Particular Reference to the Hydrological Effects of Agriculture and Forestry Practice. *Hamburg Symposium, August 1983*. Hamburg, IAHS Publ. no. 140).
- LEENDERS, J. K., WAGEMEKER, J., ROELEVINK, A., RIENTJES, T. H. M. & PARODI, G. (2009) Development of a damage and casualties tool for river floods in northern Thailand. IN

- SAMUELS (Ed.) *Flood Risk Management: Research and Practice*. London, Taylor and Francis Group.
- MADDOX, R. A., CANOVA, F. & R., H. L. (1980) Meteorological Characteristics of Flash Flood Events over the Western United States *Monthly Weather Review*, 108, 1866-1877.
- MORADKHANI, H. & SOROOSHIAN, S. (2009) General Review of Rainfall-Runoff Modeling: Model Calibration, Data Assimilation, and Uncertainty Analysis. IN SOROOSHIAN, S., HSU, K.-L., COPPOLA, E., TOMASSETTI, B., VERDECCHIA, M. & VISCONTI, G. (Eds.) *Hydrological Modeling and the water Cycle* Berlin, Springer.
- NCRS MO6 Guide for Determining Ksat Limits from Traditional Permeability Classes. IN (NCRS), **N. R. C. S.** (Ed.).
- NORBIATO, D., BORGA, M., ESPOSTI, S. D., GAUME, E. & ANQUETIN, S. (2008) Flash flood warning based on rainfall thresholds and soil moisture conditions: An assessment for gauged and ungauged basins. *Journal of Hydrology*, 362, 274-290.
- PRANCHANSRI, S. (2007) Analysis of Soil and Land cover parameters for Flood hazard assessment; A case study of the Nam chun Watershed, Phetchabun, Thailand. *Earth System Analysis* Enschede, International Institute for Geo-Information Science and Earth observation (ITC).
- RIENTJES, T. H. M. (2004) Inverse Modelling of the rainfall-runoff relation. a multi objective model calibration approach.
- SMITH, K. & WARD, R. (1998) *Floods - physical processes and human impacts*, Chichester., John Wiley and Sons.
- SOROOSHIAN, S. (1997) The Trials and Tribulations of Modeling and Measuring in Surface Water Hydrology. IN SOROOSHIAN, S., GUPTA, H. V. & RODDA, J. C. (Eds.) *Land surface Processes in hydrology. Trials and Tribulations of Modeling and Measuring*. Berlin, Springer.
- VAN DIJK, A. I. J. M. & BRUIJNZEEL, L. A. (2001) Modelling rainfall interception by vegetation of variable density using an adapted analytical model. Part 1. Model description. *Journal of Hydrology*, 247, 230-238.
- WAGENER, T., MCINTYRE, N., LEES, M. J., WHEATER, H. S. & GUPTA, H. V. (2003) Towards reduced uncertainty in conceptual rainfall-runoff modelling: Dynamic identifiability analysis. *Hydrological Processes*, 17, 455-476.
- WANG, Y. C., CHEN, S. T., YU, P. S. & YANG, T. C. (2008) Storm-event rainfall-runoff modelling approach for ungauged sites in Taiwan. *Hydrological Processes*, 22, 4322-4330.

Appendices

Appendix 3.1

The PCRaster Script

```

#! --lddin --matrixtable
#####
# PCRASTER script for the generation of a LISEM input database      #
# Rainfall runoff modelling for yen bai, vietnam                    #
# Ezra Pedzisi 21/12/09                                           #
# LISEM Script                                                    #
#####

binding
#####
### input maps ###
#####
# digital elevation model, area must be <= mask
dem = dem.map;
# field id's
fields = landuse.map;
# road mask map, not part of land use
road = roadwidt.map;
# texture/soil map
texture = soils.map;
# mask for channel maps
chanmask=chanmask.map;
# mask for the area
mask = mask.map;

#####
### input tables ###
#####
# table with crop and soil parameters for each field id
unittbl = unitsbase2.tbl;

# unitbase2 table layout #
#-----#
# 01 ksat (mm/h)
# 02 porosity (cm3/cm3)
# 03 psi initial (cm)
# 04 initial moisture content (cm3/cm3)
# 05 RR (cm)
# 06 Manning's n (-)

```

```

# 07 surface cover (-)      s
# 08 Crop height (m)
# 09 LAI m2/m2)

#####
### input constants ###
#####

Soildepth = 1000;
Chancoh = 10;
Chanman = 0.05;
Chanside = 0;
Chanwidth = 1;
Hardsurf = 0;
#####
### output maps  ###
#####

# basic topography related maps
Ldd = ${1}ldd.map;
# Local Drain Direction
area = ${1}area.map;
# reference map for Lisem
grad = ${1}grad.map;
# max slope
id = ${1}id.map;
# pluviograph influence zones
outlet = ${1}outlet.map;
# location outlets and checkpoints

# impermeable roads
roadwidth = ${1}roadwidt.map;

# crop maps
coverc=${1}per.map;
lai=${1}lai.map;
cropheight=${1}ch.map;

# soil maps
ksat=${1}ksat1.map;
psi=${1}psi1.map;
pore=${1}thetas1.map;
thetai=${1}thetai1.map;
soildep=${1}soildep1.map;

```

```

# surface maps
rr=${1}rr.map;
mann=${1}n.map;
stone=${1}stonefrc.map;
# crusted fraction, only used when option chosen in LISEM
crust=${1}crustfrc.map;
comp=${1}compfrc.map;

# channel maps
lddchan = ${1}lddchan.map;
chanwidth = ${1}chanwidt.map;
changrad = ${1}changrad.map;
chanman = ${1}chanman.map;
chanside = ${1}chanside.map;
chancoh = ${1}chancoh.map;

areamap

# MASK
dem;

initial

#####
### BASE MAPS   ###
#####

# correct topo for local depressions
report Ldd = lddcreate (dem, 1e20,1e20,1e20,1e20);
report outlet = pit(Ldd);
report outpoint = pit(Ldd.map);

# reference catchment boundaries, based on watershed from outlet
report area = catchment(Ldd, outlet);

# sine gradient (-), make sure slope > 0.001
report grad = max(sin(atan(slope(dem))),0.001);

#####
### MAPS WITH RAINFALL INFLUENCE ZONE ###
#####

report id = nominal(scalar(area)*mask.map);

```

```

#####
### CROP MAPS   ###
#####

# fraction soil cover (including residue)
report coverc = lookupscalar(unittbl, 7, fields)*mask.map;

# crop height (m)
report cropheight = lookupscalar(unittbl, 8, fields)*mask.map;

# LAI (m2/m2)
report lai = lookupscalar(unittbl, 9, fields)*mask.map;

#####
### INFILTRATION MAPS for option one layer GREEN & AMPT ###
#####

report ksat = lookupscalar(unittbl, 1, fields)*mask.map;
report pore = lookupscalar(unittbl, 2, fields)*mask.map;
report psi = abs(lookupscalar(unittbl, 3, fields))*mask.map;
report thetai = lookupscalar(unittbl, 4, fields)*mask.map;
report soildep1.map = Soildepth*mask.map;
report stonefrc.map=0*mask.map;
report hardsurf.map=0*mask.map;
## note that where the thetai1 is > thetas1, 0.8 of the latter was assigned to the former since the
former cannot be larger than the latter
#####
### SOIL SURFACE MAPS   ###
#####

# micro relief, random roughness (=std dev in cm)
report rr = max(lookupscalar(unittbl, 5, fields)*mask.map,0.01);

# Manning's n (-)
# take from table
report mann = lookupscalar(unittbl, 6, fields)*mask.map;

# or use simple regression from Limburg data: CAREFULL this is bullshit
# report mann = 0.0132*rr+0.01803*coverc+0.072;

report stonefrc = 0*mask.map;

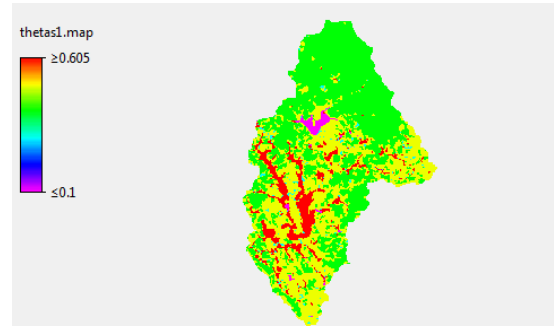
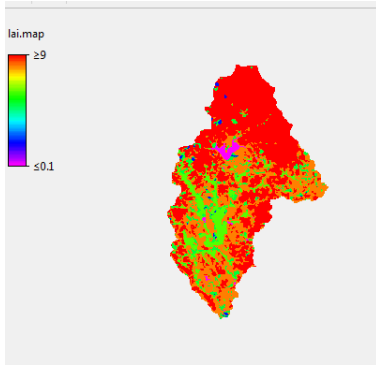
#####
### CHANNEL MAPS   ###

```

```
#####  
report lddchan=lddcreate(dem*chanmask.map,1e20,1e20,1e20,1e20);  
report changrad=max(0.001,sin(atan(slope(chanmask*dem))))*mask.map;  
report chancoh=chanmask*scalar(Chancoh)*mask.map;  
report chanman=chanmask*scalar(Chanman)*mask.map;  
report chanside=chanmask*scalar(Chanside)*mask.map;  
report chanwidth=chanmask*scalar(Chanwidth)*mask.map;  
  
report roadwidth = road*mask.map;  
# copy the road map to the 1 directory
```

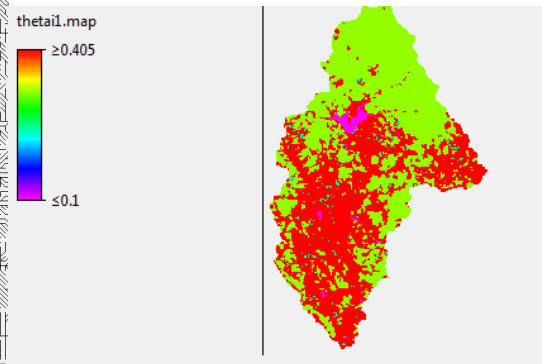
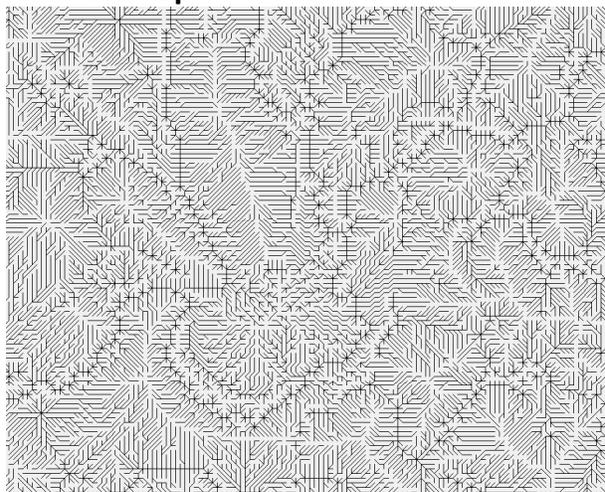
Appendix 3.2: Maps for LISEM model

lai map



Porosity map

Idd map



initial soil moisture content map

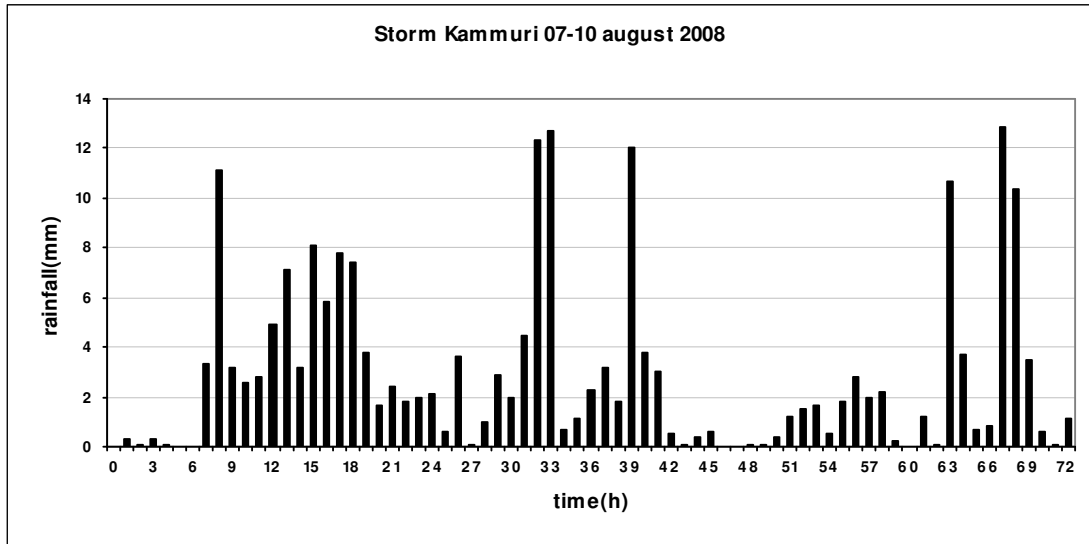
Appendix 3.3: Cross section measurement



Fig. 1 shows the stages in setting up and measuring of the spill-way cross section at the reservoir upstream of the catchment. The stages were; setting up the measuring lines (a-d), stretching the lines (e - f), and the actual depth measurement process (g - h).(source: fieldwork photographs September 2009).

Appendix3.5: Rainfall data

year	max daily rainfall	rank	lef Prob	TR	y
1977	17.0	1	0.03	1.03	-1.31
1973	30.7	2	0.05	1.05	-1.10
1988	37.5	3	0.08	1.08	-0.95
1978	37.7	4	0.10	1.11	-0.83
1983	40.8	5	0.13	1.14	-0.73
1999	41.1	6	0.15	1.18	-0.64
1984	41.3	7	0.18	1.21	-0.56
1993	41.5	8	0.20	1.25	-0.48
1964	41.7	9	0.23	1.29	-0.40
1981	42.5	10	0.25	1.33	-0.33
1962	43.3	11	0.28	1.38	-0.26
1963	47.0	12	0.30	1.43	-0.19
1969	48.7	13	0.33	1.48	-0.12
1985	49.7	14	0.35	1.54	-0.05
1966	55.0	15	0.38	1.60	0.02
1979	55.7	16	0.40	1.67	0.09
1991	58.5	17	0.43	1.74	0.16
1989	59.0	18	0.45	1.82	0.23
1982	59.3	19	0.48	1.90	0.30
1972	60.8	20	0.50	2.00	0.37
1992	61.0	21	0.53	2.11	0.44
1970	61.3	22	0.55	2.22	0.51
1967	65.1	23	0.58	2.35	0.59
1968	68.1	24	0.60	2.50	0.67
1986	77.5	25	0.63	2.67	0.76
2001	78.0	26	0.65	2.86	0.84
1971	78.2	27	0.68	3.08	0.93
1987	80.8	28	0.70	3.33	1.03
1980	87.0	29	0.73	3.64	1.13
1994	90.0	30	0.75	4.00	1.25
1990	94.5	31	0.78	4.44	1.37
2000	100.0	32	0.80	5.00	1.50
2004	101.0	33	0.83	5.71	1.65
2008	135.0	34	0.85	6.67	1.82
2002	137.0	35	0.88	8.00	2.01
2003	139.0	36	0.90	10.00	2.25
2005	141.0	37	0.93	13.33	2.55
2006	181.0	38	0.95	20.00	2.97
1965	261.8	39	0.98	40.00	3.68



Storm Kammuri of 2008 August 07-13

Appendix3.6: Additional info



Activities in the field: Interviewing the local farmers, top, cross section measurement, field consultation, upstream diver location, Ksat experiment and depth measurement